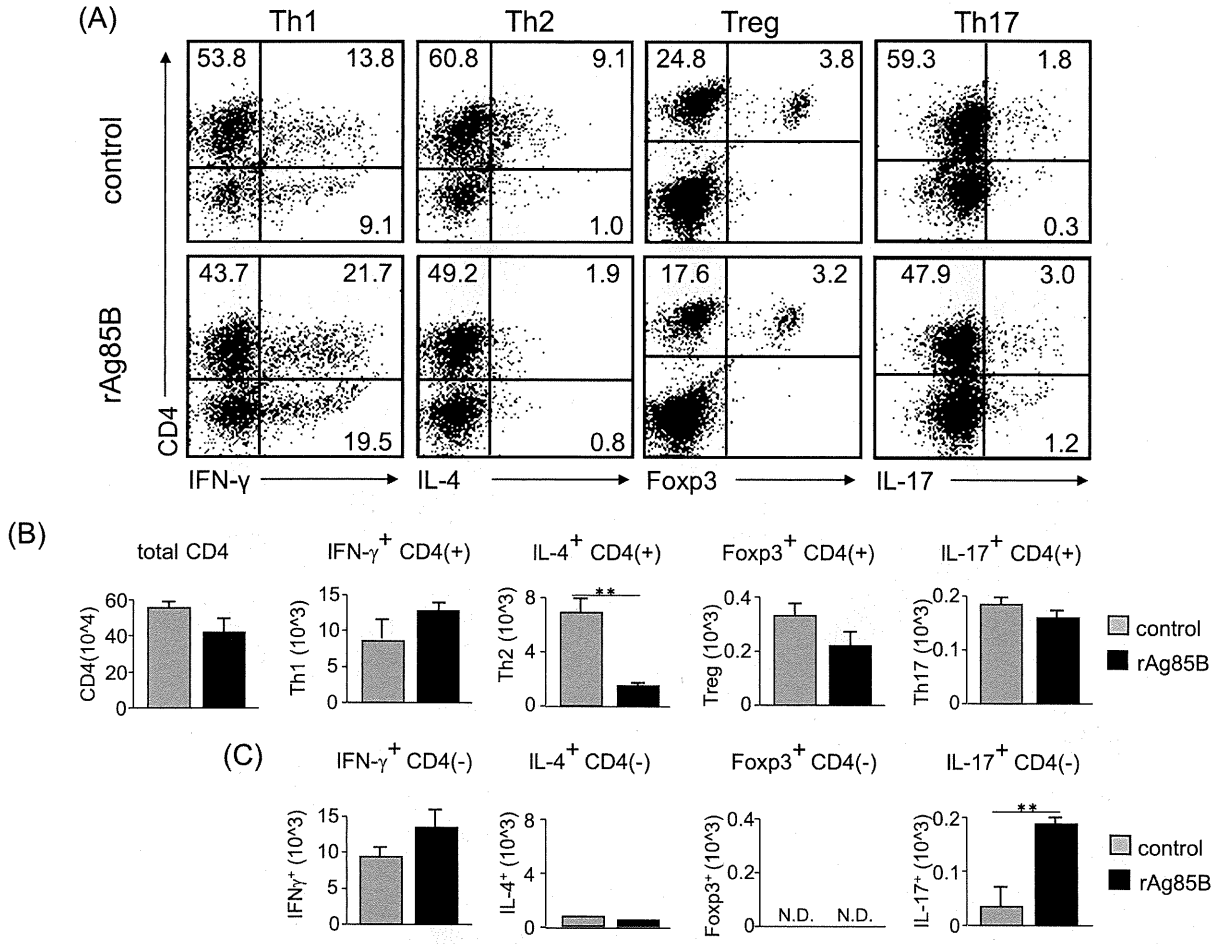

Figure 5. IFN-γ and IL-17-producing CD4-negative cell subsets proliferated in BAL fluid after rAg85B administration. OVA-immunized (i.p., day0 and 14) and sensitized (5% aerosolized-OVA, day21 to 25) BALB/c mice were challenged with PBS or rAg85B protein (i.p. (100 μg; days 0 and 14) and i.n. (20 μg; days 21, 23, and 25)). At 24 h after the last OVA sensitization, BAL fluid from naïve or OVA sensitized BALB/c mice treated with PBS or rAg85B, were harvested. BAL cells were stimulated with ionomycin and PMA for 5 h, and with brefeldin A added in the last 3 h. Flow cytometry of stimulated BAL cells from PBS-treated (upper) and rAg85B protein-treated (lower) OVA-sensitized mice stained with specific antibodies indicated marker. Numbers in quadrants indicate percent of cells in each (*A*). Absolute numbers of various cell populations (above graphs) in BAL fluid (*B*, *C*). Data are representative of three independent experiments (**P<0.01 compared with OVA control. error bars, s.d.; n = 6 mice).
doi:10.1371/journal.pone.0106807.g005

produce IL-17 in certain conditions, the numbers of these IL-17-secreting cells in BAL fluid from rAg85B-administered mice showed little or no change compared with those in the control group in our experimental setting. Remarkably, these responses induced by rAg85B were observed in allergic animals but not in naïve ones (data not shown).

Functions of IL-17 and IL-22 in rAg85B-administered mice

We next investigated the importance of Th17-related cytokines by using neutralizing antibodies (Abs) to IL-17 and IL-22 in rAg85B-administered experimental mice. Administration of neutralizing Abs to IL-17 and IL-22 did not show any systemic inhibitory effects induced by rAg85B as a result of IgE production (Fig. 7*A*). Furthermore, neutralization of IL-17 and IL-22 did not restore the functions of rAg85B with immune deviation from a disease-promoting Th2 response towards a Th1 response, whereas inhibition of TARC production regulated by rAg85B was reversed by neutralizing IL-22 Abs treatment (Fig. 7*B*). These results suggested that IL-17 and IL-22 induced by rAg85B have little or no systemic inhibitory effect on the development of allergic inflammation in the lung. Neutralization of IFN-γ at the challenge phase also had little or no suppressive effect on serum IgE expressions and eosinophilia induced by rAg85B treatment. (data not shown). The number of infiltrating cells in BAL fluid were also not changed in mice administered neutralizing Abs to IL-17 and IL-22 (Fig. 7*C*); however, fractions of infiltrating cells in BAL fluid were different. Neutralization of IL-17 by IL-17-specific Abs prevented neutrophil infiltration by rAg85B administration in the airway, and this preventive effect on infiltration of neutrophils was partial in IL-22-specific Abs administered mice (Fig. 7*D*). Eosinophilia suppression by rAg85B administration was reversed by neutralizing IL-22 Abs treatment (Fig. 7*D*). These results parallel previous observations of the specificity of IL-17 and IL-22 effects [20]. Enhancement of innate immune cell recruitment induced by rAg85B was fully reversed by neutralizing IL-17 Abs treatment, and this rAg85B effect was partially reversed by administration of neutralizing IL-22 Abs in γδT cells (Fig. 7*D*). These results showed that Th17-related cytokines induced by rAg85B have pivotal roles in innate immune cell recruitment in BAL fluid and in severity of

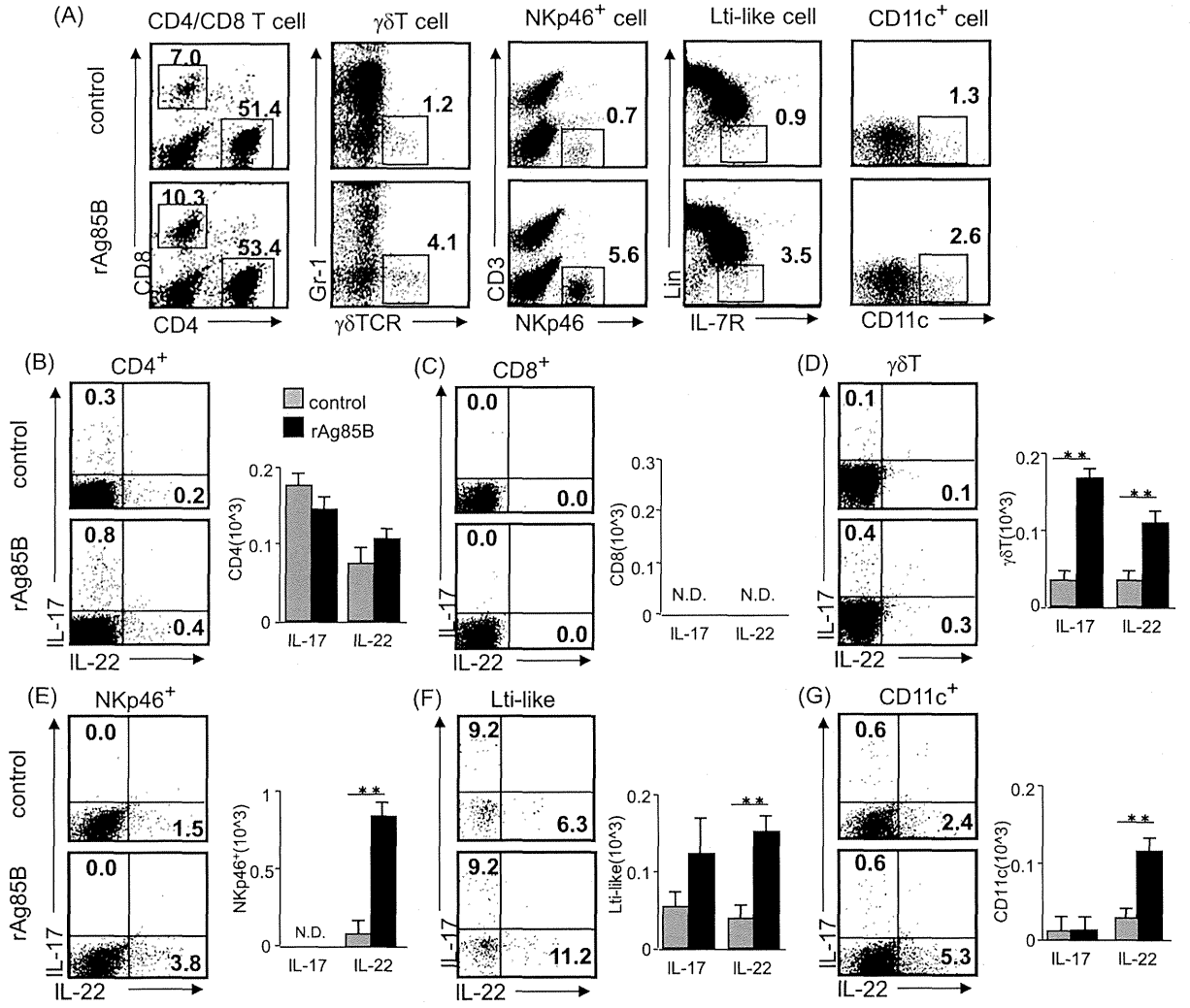

Figure 6. Innate immune cells that secrete Th17-related cytokines are induced by rAg85B administration in BAL fluid. OVA-immunized (i.p., day0 and 14) and sensitized (5% aerosolized-OVA, day21 to 25) BALB/c mice were challenged with PBS or rAg85B protein (i.p. (100 μg; days 0 and 14) and i.n. (20 μg; days 21, 23, and 25)). At 24 h after the last OVA sensitization, BAL fluid from naïve or OVA sensitized BALB/c mice treated with PBS or rAg85B, were harvested. BAL cells were stimulated with ionomycin and PMA for 5 h, and with brefeldin A added in the last 3 h. Flow cytometry of BAL cells from PBS-treated (upper) and rAg85B protein-treated (lower) OVA-sensitized mice stained with anti-CD3, anti-CD4, anti-CD8, anti-Gr-1, anti-γδ TCR, anti-NKp46, anti-CD11c, anti-CD127 (IL-7R) and Lineage specific marker (CD3, CD19, Gr-1, CD11b, CD11c). Numbers in quadrants indicate percent of cells in each (*A*). Intracellular IL-17 and IL-22 staining in indicated cells by flow cytometry (dot plots) and absolute numbers of those cell populations (side graphs) in the BAL fluid (*B, C, D, E, F, G*). Data are representative of at least two independent experiments (**P<0.01 compared with OVA control. error bars, s.d.; n = 6 mice).
doi:10.1371/journal.pone.0106807.g006

lung inflammation but not in regulated systemic allergic inflammation involving Th responses.

Administration of rAg85B promoted Th17-related innate responses in the lung

Our data suggested an important link between rAg85B and airway innate immune cells producing IL-17 and IL-22 that contributed to the homeostasis expression of Th17-related cytokine response genes. However, these two cytokines induced by rAg85B administration did not clearly show inhibitory effects on systemic allergy responses (Fig. 7*A*, 7*B*). From these findings, we next explored the relationship between the roles of airway innate immune cells and wound repair in mice that received i.n. administration of rAg85B. Mice that received IL-17 or IL-22 or both neutralizing antibodies showed a marked induction of fibrosis and actin staining but incomplete cancellation of rAg85B suppressive effects at the same levels as those in OVA control mice (Fig. 8*A*). Histological findings suggested that IL-17 and IL-22 induced by rAg85B i.n. administration were partially involved in regulation of local tissue allergic inflammation. The inhibition of rAg85B effects by neutralizing Abs of IL-17 and IL-22 to allergic inflammation was partial; however, tissue repair in lungs was seen in rAg85B-administered mice by histopathological examination. These results led us to hypothesize that IL-17 and IL-22 induced by rAg85B induced local tissue remodeling/repair molecules. To confirm this, the induction of tissue homeostasis-related gene expression in rAg85B-administered mice was examined by real-time RT-PCR. Rb2, Cyclin D1 and c-Myc are associated with

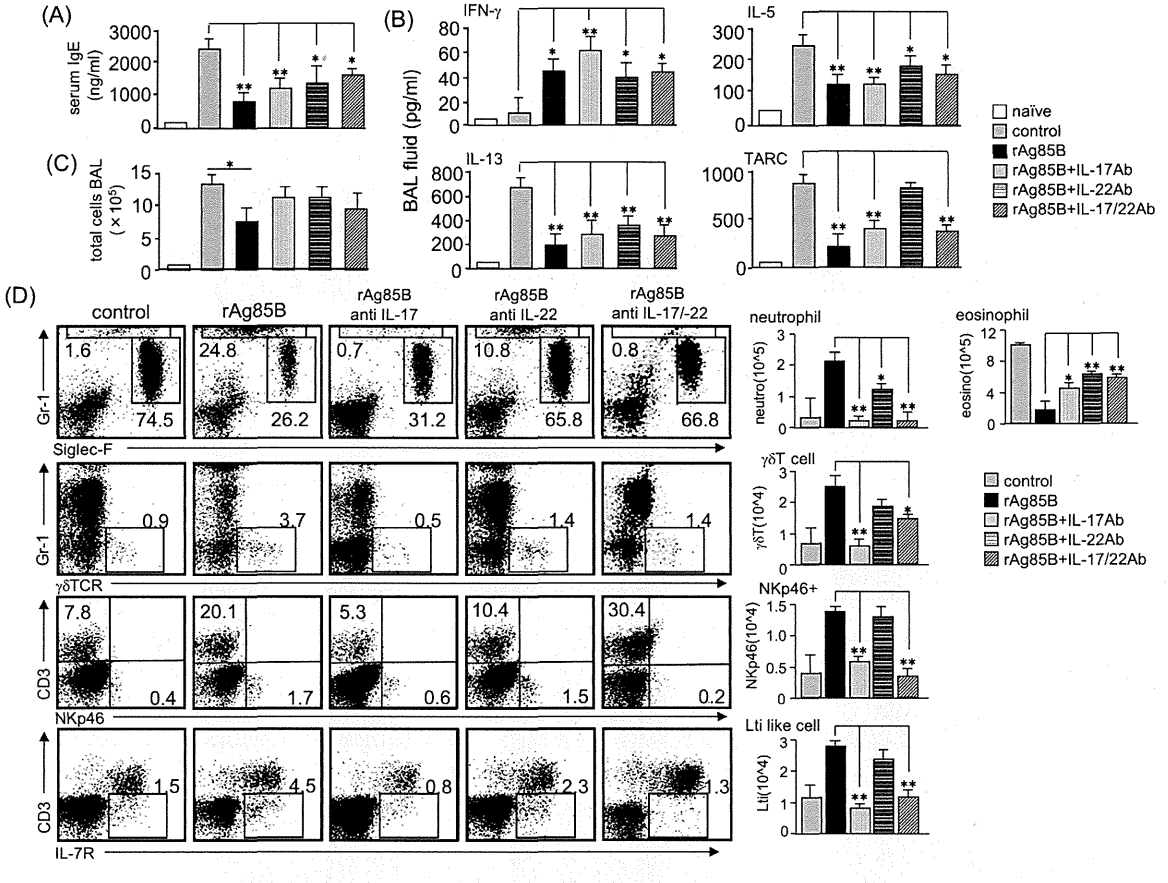

Figure 7. Neutralization of Th17-related cytokines inhibits cell recruitment to the lung but does not change cytokine and chemokine production. OVA-sensitized BALB/c mice (5% aerosolized-OVA, day21 to 25) were challenged intranasally with PBS (control), rAg85B (rAg85B + isotype-matched control antibody (Ab)), rAg85B plus neutralizing IL-17 (rAg85B + IL-17Ab) or IL-22 (rAg85B + IL-22Ab), or a combination of both antibodies (rAg85B +IL-17/22Ab) on days 21, 23, and 25. The isotype control was treated with the same time course as neutralization Ab i.n. administration. One day after the last challenge, OVA-specific serum IgE concentration and levels of cytokines and chemokines in BAL fluid were determined by ELISA (*A, B*). BAL cells from naïve or OVA sensitized BALB/c mice treated with PBS or rAg85B with/without neutralization Ab were counted (*C*), and were stained with anti-Gr-1, anti-Siglec-F, anti-gd TCR, anti-CD3, anti-NKp46, and anti-CD127 for flow cytometric analysis. Numbers adjacent to outlined area indicate percent of eosinophils (Gr-1^{dull}, Siglec-F^{+}), neutrophils (Gr-1^{+}, Siglec-F^{neg}), γδT cells (Gr-1^{neg}, γδTCR^{+}), NKp46^{+} cells (CD3^{neg}, NKp46^{+}), LTi like cells (CD3^{neg}, L-7R^{+}), and absolute numbers of those cell populations (side graphs) in BAL fluid (*D*). Data are representative of at least two independent experiments (*P<0.05, **P<0.01 compared with rAg85B+isotype control challenged group. error bars, s.d.; n = 6 mice).
doi:10.1371/journal.pone.0106807.g007

wound healing, tissue repair and remodeling including proliferative molecules [21]. Muc1 [22,23], matrix metalloproteinase 13 (MMP13) [24], and the extracellular matrix proteins decorin and dermatopontin [25] produce protective mucus. Lymphotoxin-beta (Ltb) is a molecule related to signaling in stromal cells to produce factors that organize lymphoid cells into lymph nodes [26]. The transcription of Reg3γ is involved in tissue repair and antimicrobial responses [27]. The expression of these genes involved in innate immune response-mediated signaling was significantly enhanced in the lungs of rAg85B-administered mice (Fig. 8*B*). The increases in mRNA levels of all molecules other than Reg3γ and dermatopontin were inhibited by treatment with neutralizing Abs of IL-17 (Fig. 8*B*). On the other hand, the expression of mRNA of molecules enhanced by rAg85B administration was decreased after treatment with IL-22 neutralizing Abs except for Rb2, Cyclin D1, c-Myc, Mmp13 and Muc1 (Fig. 8*B*). These results suggested that IL-17 and IL-22 induced by rAg85B administration affected induction of pulmonary innate response. In conclusion, IL-17 induced by rAg85B administration induced the expression of various types of wound healing, tissue repair and remodeling molecules. Interestingly, IL-22 in rAg85B-immunized mice induces the expression of molecules mainly associated antimicrobial responses such as Reg3γ, decorin, dermatopontin and Ltb. In summary, Th1 and Th17 cells are induced in regional lymph nodes by administration of rAg85B; however, Th17 cells are not induced in BAL unlike in Th1 cells. IL-17 is produced by innate immune cells with IL-22 production. IL-17 and IL-22 are important in not only anti-allergic effects, such as eosinophil inhibition, but also wound healing and tissue repair in the lung (Fig. 9).

Discussion

Results of several experimental studies on mycobacteria involving mycobacterial antigens in mouse models of allergic airway inflammation have been reported. In murine asthma models, intranasal administration of BCG suppressed asthma manifestations probably through Th1 response [2,4], Treg cells [5,6,28], or NKT cells [7,8,29]. In our experimental setting using rAg85B protein, we did not find any detectable effect or

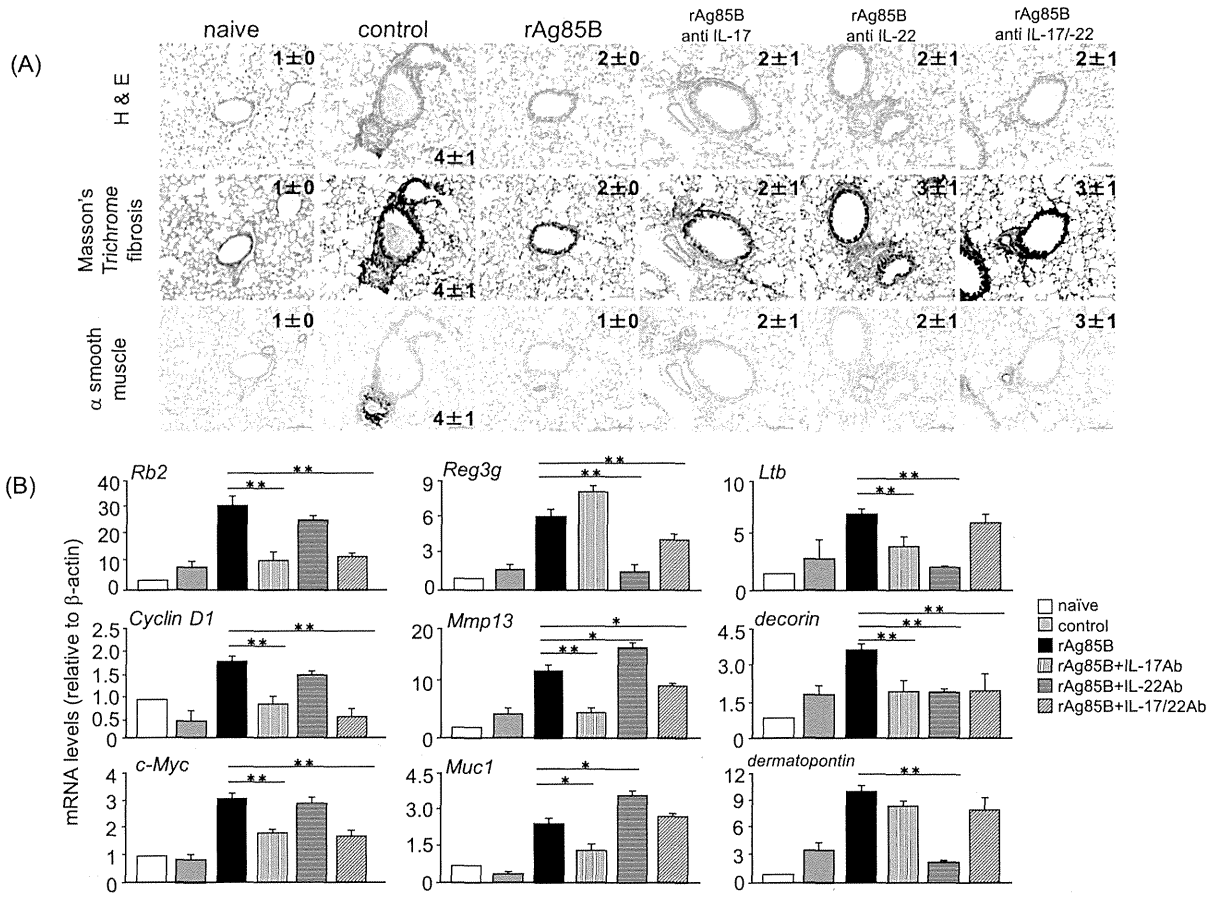

Figure 8. Ag85B administration promotes Th17-related innate responses in the lung. OVA-sensitized BALB/c mice (5% aerosolized-OVA, day21 to 25) were challenged intranasally with PBS (control), rAg85B (rAg85B + isotype control), rAg85B plus neutralizing IL-17 (rAg85B + IL-17Ab) or IL-22 (rAg85B + IL-22Ab), or a combination of both antibodies (rAg85B +IL-17/22Ab) on days 21, 23, and 25. The isotype-matched control antibody was treated with the same time course as neutralization Ab i.n. administration. Lungs from naïve or OVA sensitized BALB/c mice treated with PBS or rAg85B with/without neutralization Ab were sampled one day after the last challenge for histological analysis and quantification of mRNA levels. Lung sections were stained with hematoxylin and eosin (left row, scale bar, 100 mm), Masson's trichrome (center row, scale bar, 100 mm), α-smooth muscle actin (right row, scale bar, 50 mm). Numbers in quadrants indicate the score scale from 0 to 5 in each (*A*). Real-time RT-PCR was performed for the indicated molecules expression on RNA isolated from individual mice lungs (*B*). Data are representative of at least two independent experiments (*P<0.05, **P<0.01 compared with rAg85B+isotype control challenged group. error bars, s.d.; n = 6 mice).
doi:10.1371/journal.pone.0106807.g008

substantial change in numbers of both NKT cells and Treg cells in BAL fluid from rAg85B-administered mice. Moreover, microarray analysis revealed that the gene expression pattern of splenocytes stimulated with rAg85B and that of splenocytes stimulated with BCG were very different (data not shown). This discrepancy in the effects of vaccination with BCG and vaccination with rAg85B might be related to the factors affecting immune responses. BCG contains many essential components to induce early immune response such as glycolipid and DNA, whereas rAg85B is a single immunogenic protein.

The present study indicated that Th17-related immune responses induced by rAg85B administration had a suppressive effect on allergic airway inflammation, and we attributed this suppressive effect to the larger proportion of Th17-related cytokine-producing innate immune cells in BAL fluid. It has been reported that Mycobacterium antigens increased the number of γδT cells that express IFN-γ [30] or IL-17 [31], and these responses induce healing to epithelial surfaces [32]. Given the integral role of γδT cells in innate immunity, γδT cells are one of the crucial factors in the rAg85B immune regulatory functions. Interestingly, our study also showed that IL-22-producing cells in lungs of rAg85B-administered mice were $NKp46^+$ cells, LTi-like cells, γδT cells and $CD11c^+$ cells. This is the first time demonstration of an important link between the mycobacterium antigen rAg85B and IL-22-producing cells. Although we could not rule out the possibility of Th17 cytokine-producing cells other than those described here, $NKp46^+$ cells, LTi-like cells, γδT cells and $CD11c^+$ cells were thought to be rapid innate sources of IL-22, which is required in the early stage to maintain epithelial cell integrity and to suppress eosinophilia. Moreover, IL-22 can act synergistically or additively with other cytokines, including IL-17 or TNF, to promote gene expression for antimicrobial peptides, chemokines, matrix metalloproteinases, cytokines, and acute-phase proteins from epithelial cells in the lung [33]. These findings also support our results showing that simultaneous induction of these cytokines and expression of many genes may be beneficial functions of rAg85B treatment in local allergic pathology.

Pulmonary infection of mycobacteria induced not only a neutrophil-mediated response but also T cell-mediated IFN-γ

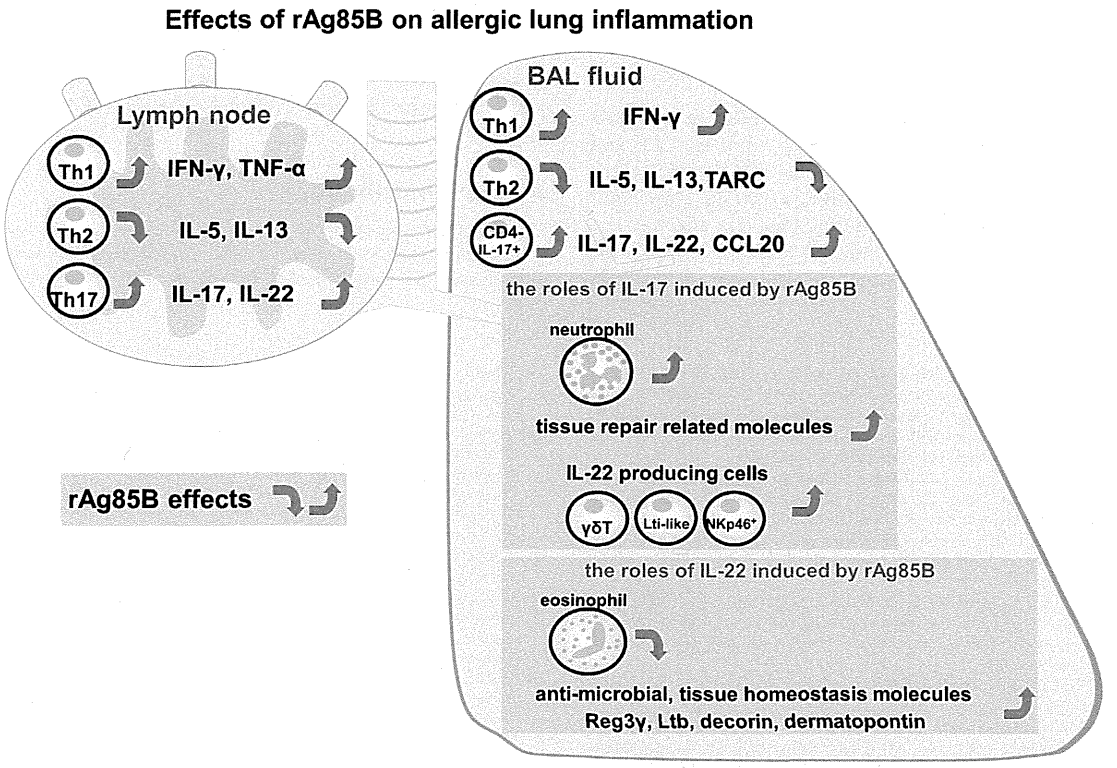

Figure 9. Schematic illustration of the proposed effects of rAg85B in a mouse model of allergic inflammation. IFN-γ and IL-17-producing Th cells are induced in regional lymph nodes by rAg85B challenge, however, Th17 cells do not enter the lung unlike Th1 cells. Th17-related cytokine-secreting cells in lungs from rAg85B-administered mice are innate immune cells including γδT cells, IL-7R$^+$ Lin$^-$ cells, CD3$^-$ NKp46$^+$ cells and CD11c$^+$ cells. IL-17 and IL-22 induced by rAg85B in an allergic environment have crucial roles in not only anti-allergic effects but also regulation of tissue homeostatic reactions.
doi:10.1371/journal.pone.0106807.g009

production and granuloma formation depending on IL-17 from especially γδT cells [34]. The hallmark of mycobacterial infection in the lung is granuloma formation with infiltrating neutrophils, which creates an immune microenvironment in which the infection can be controlled. On the other hand, it also provides the mycobacterium with a niche in which it can survive, modulating the immune response to ensure its survival without damage over a long period of time [35,36]. Mature granulomas include fibroblasts and extracellular matrix, which surround and separate the granulomas from the normal environment. Administration of anti-IL-17 Abs during the inhalatory challenge phase abolished the bronchial neutrophilia and the upregulation of genes related to tissue repair and homeostasis observed in rAg85B-administered mice in the present study. Neutrophils may also promote epithelial healing [37] and are now known to be rich sources of prestored and expressible proteins [38] that may directly promote wound healing [39,40]. In the present study, induction of neutrophilia and upregulation of described genes related to wound healing with suppression of tissue injury might be the mechanisms of granuloma formulation induced by mycobacteria infection.

In the present study, IFN-γ and Th17-related cytokines were key factors to regulate allergic severity in our experimental setting. Although infiltration of Th1 and Th17 cells elicited by rAg85B was induced in pulmonary lymph nodes, such effector cells were not increased in BAL fluid of mice showing anti-allergic effects of Ag85B administration. Moreover, our results suggested that the accumulation of neutrophils and IL-17 and/or IL-22-producing innate immune cells contributed to the homeostatic functions in the Th1-balanced environment induced by rAg85B administration. These findings provide a new insight into the regulatory effects of various innate immune factors induced by the mycobacteria major secretion protein rAg85B in allergic inflammation.

Supporting Information

Figure S1 SDS-PAGE separation and silver staining of rAg85B. The recombinant purified Ag85B was solubilized in sample buffer to the desired concentration, and boiled for 5 min. 15 μl/well from each samples were separated on 10% SDS gel using mini-PROTEAN electrophoresis instrument (Bio-Rad Laboratories). Silver staining of the gel was performed according to the standard protocol of EzStain Silver (ATTO). Various concentration of rAg85B on the gel (12.5, 25, 50, 100, 200, and 400 ng).
(TIF)

Figure S2 CD4$^+$ Foxp3$^+$ T cells were almost expressing CD25. OVA-immunized (i.p., day0 and 14) and sensitized (5% aerosolized-OVA, day21 to 25) BALB/c mice were challenged with PBS or rAg85B protein (i.p. (100 μg; days 0 and 14) and i.n. (20 μg; days 21, 23, and 25)). At 24 h after the last OVA sensitization, mediastinal lymph nodes (MLNs) from naïve or OVA sensitized BALB/c mice treated with PBS or rAg85B, were harvested. MLNs cells from naïve (upper), PBS-treated (middle) and rAg85B protein-treated (lower) OVA-sensitized mice were

stained with anti-CD4 and anti-Foxp3. Cells in R1-R4 were analyzed for the expression of CD25.
(TIF)

Figure S3 The composition of BAL cells in rAg85B administered mice. OVA-immunized (i.p., day0 and 14) and sensitized (5% aerosolized-OVA, day21 to 25) BALB/c mice were challenged with PBS (control) or rAg85B (i.p. (100 μg; days 0 and 14) and i.n. (20 μg; days 21, 23, and 25)). One day after the last challenge, BAL cells from OVA sensitized BALB/c mice treated with PBS or rAg85B were counted. Different BAL cells populations were measured by surface staining. Flow cytometry of BAL cells stained with anti-CD3, anti-CD4, anti-CD8, anti-Gr-1, anti-γδ TCR, anti-NKp46, anti-CD11c, anti-CD127 (IL-7R) and Lineage specific marker (CD3, CD19, Gr-1, CD11b, CD11c).
(TIF)

Author Contributions

Conceived and designed the experiments: YY. Performed the experiments: YT HI MY. Analyzed the data: YY KM. Contributed reagents/materials/analysis tools: TF. Contributed to the writing of the manuscript: YT YY.

References

1. Adams JF, Scholvinck EH, Gie RP, Potter PC, Beyers N, et al. (1999) Decline in total serum IgE after treatment for tuberculosis. Lancet 353: 2030–2033.
2. Herz U, Gerhold K, Gruber C, Braun A, Wahn U, et al. (1998) BCG infection suppresses allergic sensitization and development of increased airway reactivity in an animal model. J Allergy Clin Immunol 102: 867–874.
3. Cavallo GP, Elia M, Giordano D, Baldi C, Cammarota R (2002) Decrease of specific and total IgE levels in allergic patients after BCG vaccination: preliminary report. Arch Otolaryngol Head Neck Surg 128: 1058–1060.
4. Choi IS, Koh YI (2002) Therapeutic effects of BCG vaccination in adult asthmatic patients: a randomized, controlled trial. Ann Allergy Asthma Immunol 88: 584–591.
5. Stassen M, Jonuleit H, Muller C, Klein M, Richter C, et al. (2004) Differential regulatory capacity of CD25+ T regulatory cells and preactivated CD25+ T regulatory cells on development, functional activation, and proliferation of Th2 cells. J Immunol 173: 267–274.
6. Robinson DS, Larche M, Durham SR (2004) Tregs and allergic disease. J Clin Invest 114: 1389–1397.
7. Cui J, Watanabe N, Kawano T, Yamashita M, Kamata T, et al. (1999) Inhibition of T helper cell type 2 cell differentiation and immunoglobulin E response by ligand-activated Valpha14 natural killer T cells. J Exp Med 190: 783–792.
8. Harada M, Magara-Koyanagi K, Watarai H, Nagata Y, Ishii Y, et al. (2006) IL-21-induced Bepsilon cell apoptosis mediated by natural killer T cells suppresses IgE responses. J Exp Med 203: 2929–2937.
9. Torrado E, Cooper AM (2010) IL-17 and Th17 cells in tuberculosis. Cytokine Growth Factor Rev 21: 455–462.
10. Griffiths KL, Pathan AA, Minassian AM, Sander CR, Beveridge NE, et al. (2011) Th1/Th17 cell induction and corresponding reduction in ATP consumption following vaccination with the novel Mycobacterium tuberculosis vaccine MVA85A. PLoS One 6: e23463.
11. Lambrecht BN, Hammad H (2012) The airway epithelium in asthma. Nat Med 18: 684–692.
12. Holgate ST (2012) Innate and adaptive immune responses in asthma. Nat Med 18: 673–683.
13. Sonnenberg GF, Fouser LA, Artis D (2011) Border patrol: regulation of immunity, inflammation and tissue homeostasis at barrier surfaces by IL-22. Nat Immunol 12: 383–390.
14. Takamura S, Matsuo K, Takebe Y, Yasutomi Y (2005) Ag85B of mycobacteria elicits effective CTL responses through activation of robust Th1 immunity as a novel adjuvant in DNA vaccine. J Immunol 175: 2541–2547.
15. Mori H, Yamanaka K, Matsuo K, Kurokawa I, Yasutomi Y, et al. (2009) Administration of Ag85B showed therapeutic effects to Th2-type cytokine-mediated acute phase atopic dermatitis by inducing regulatory T cells. Arch Dermatol Res 301: 151–157.
16. Karamatsu K, Matsuo K, Inada H, Tsujimura Y, Shiogama Y, et al. (2012) Single systemic administration of Ag85B of mycobacteria DNA inhibits allergic airway inflammation in a mouse model of asthma. J Asthma Allergy 5: 71–79.
17. Takatori H, Kanno Y, Watford WT, Tato CM, Weiss G, et al. (2009) Lymphoid tissue inducer-like cells are an innate source of IL-17 and IL-22. J Exp Med 206: 35–41.
18. Cella M, Fuchs A, Vermi W, Facchetti F, Otero K, et al. (2009) A human natural killer cell subset provides an innate source of IL-22 for mucosal immunity. Nature 457: 722–725.
19. Korn T, Bettelli E, Oukka M, Kuchroo VK (2009) IL-17 and Th17 Cells. Annu Rev Immunol 27: 485–517.
20. Schnyder B, Lima C, Schnyder-Candrian S (2010) Interleukin-22 is a negative regulator of the allergic response. Cytokine 50: 220–227.
21. Dieli F, Ivanyi J, Marsh P, Williams A, Naylor I, et al. (2003) Characterization of lung gamma delta T cells following intranasal infection with Mycobacterium bovis bacillus Calmette-Guerin. J Immunol 170: 463–469.
22. Sonnenberg GF, Nair MG, Kirn TJ, Zaph C, Fouser LA, et al. (2010) Pathological versus protective functions of IL-22 in airway inflammation are regulated by IL-17A. J Exp Med 207: 1293–1305.
23. Sugimoto K, Ogawa A, Mizoguchi E, Shimomura Y, Andoh A, et al. (2008) IL-22 ameliorates intestinal inflammation in a mouse model of ulcerative colitis. J Clin Invest 118: 534–544.
24. Planus E, Galiacy S, Matthay M, Laurent V, Gavrilovic J, et al. (1999) Role of collagenase in mediating in vitro alveolar epithelial wound repair. J Cell Sci 112 (Pt 2): 243–252.
25. Monticelli LA, Sonnenberg GF, Abt MC, Alenghat T, Ziegler CG, et al. (2011) Innate lymphoid cells promote lung-tissue homeostasis after infection with influenza virus. Nat Immunol 12: 1045–1054.
26. De Togni P, Goellner J, Ruddle NH, Streeter PR, Fick A, et al. (1994) Abnormal development of peripheral lymphoid organs in mice deficient in lymphotoxin. Science 264: 703–707.
27. Graf R, Schiesser M, Reding T, Appenzeller P, Sun LK, et al. (2006) Exocrine meets endocrine: pancreatic stone protein and regenerating protein–two sides of the same coin. J Surg Res 133: 113–120.
28. Zuany-Amorim C, Sawicka E, Manlius C, Le Moine A, Brunet LR, et al. (2002) Suppression of airway eosinophilia by killed Mycobacterium vaccae-induced allergen-specific regulatory T-cells. Nat Med 8: 625–629.
29. Taniguchi M, Harada M, Kojo S, Nakayama T, Wakao H (2003) The regulatory role of Valpha14 NKT cells in innate and acquired immune response. Annu Rev Immunol 21: 483–513.
30. Dieli F, Troye-Blomberg M, Ivanyi J, Fournie JJ, Bonneville M, et al. (2000) Vgamma9/Vdelta2 T lymphocytes reduce the viability of intracellular Mycobacterium tuberculosis. Eur J Immunol 30: 1512–1519.
31. Lockhart E, Green AM, Flynn JL (2006) IL-17 production is dominated by gammadelta T cells rather than CD4 T cells during Mycobacterium tuberculosis infection. J Immunol 177: 4662–4669.
32. Li Z, Burns AR, Miller SB, Smith CW (2011) CCL20, gammadelta T cells, and IL-22 in corneal epithelial healing. FASEB J 25: 2659–2668.
33. Guilloteau K, Paris I, Pedretti N, Boniface K, Juchaux F, et al. (2010) Skin Inflammation Induced by the Synergistic Action of IL-17A, IL-22, Oncostatin M, IL-1{alpha}, and TNF-{alpha} Recapitulates Some Features of Psoriasis. J Immunol.
34. Okamoto Yoshida Y, Umemura M, Yahagi A, O'Brien RL, Ikuta K, et al. (2010) Essential role of IL-17A in the formation of a mycobacterial infection-induced granuloma in the lung. J Immunol 184: 4414–4422.
35. Adams DO (1976) The granulomatous inflammatory response. A review. Am J Pathol 84: 164–192.
36. Sandor M, Weinstock JV, Wynn TA (2003) Granulomas in schistosome and mycobacterial infections: a model of local immune responses. Trends Immunol 24: 44–52.
37. Li Z, Burns AR, Han L, Rumbaut RE, Smith CW (2011) IL-17 and VEGF are necessary for efficient corneal nerve regeneration. Am J Pathol 178: 1106–1116.
38. Grenier A, Chollet-Martin S, Crestani B, Delarche C, El Benna J, et al. (2002) Presence of a mobilizable intracellular pool of hepatocyte growth factor in human polymorphonuclear neutrophils. Blood 99: 2997–3004.
39. Li Z, Rumbaut RE, Burns AR, Smith CW (2006) Platelet response to corneal abrasion is necessary for acute inflammation and efficient re-epithelialization. Invest Ophthalmol Vis Sci 47: 4794–4802.
40. Stirling DP, Liu S, Kubes P, Yong VW (2009) Depletion of Ly6G/Gr-1 leukocytes after spinal cord injury in mice alters wound healing and worsens neurological outcome. J Neurosci 29: 753–764.

Citation: Molecular Therapy—Nucleic Acids (2014) 3, e168; doi:10.1038/mtna.2014.20

www.nature.com/mtna

CD4+ T Cells Modified by the Endoribonuclease MazF Are Safe and Can Persist in SHIV-infected Rhesus Macaques

Naoki Saito[1], Hideto Chono[1], Hiroaki Shibata[2], Naohide Ageyama[2], Yasuhiro Yasutomi[2] and Junichi Mineno[1]

MazF, an endoribonuclease encoded by *Escherichia coli*, specifically cleaves the ACA (adenine–cytosine–adenine) sequence of single-stranded RNAs. Conditional expression of MazF under the control of the HIV-1 LTR promoter rendered CD4+ T cells resistant to HIV-1 replication without affecting cell growth. To investigate the safety, persistence and efficacy of MazF-modified CD4+ T cells in a nonhuman primate model *in vivo*, rhesus macaques were infected with a pathogenic simian/human immunodeficiency virus (SHIV) and transplanted with autologous MazF-modified CD4+ T cells. MazF-modified CD4+ T cells were clearly detected throughout the experimental period of more than 6 months. The CD4+ T cell count values increased in all four rhesus macaques. Moreover, the transplantation of the MazF-modified CD4+ T cells was not immunogenic, and did not elicit cellular or humoral immune responses. These data suggest that the autologous transplantation of MazF-modified CD4+ T cells in the presence of SHIV is effective, safe and not immunogenic, indicating that this is an attractive strategy for HIV-1 gene therapy.
Molecular Therapy—Nucleic Acids (2014) **3**, e168; doi:10.1038/mtna.2014.20; published online 10 June 2014
Subject Category: Therapeutic proof-of-concept Gene insertion, deletion & modification

Introduction

Antiretroviral therapy (ART), which is based on a combination of different classes of inhibitors, is widely used for the treatment of human immunodeficiency virus type 1 (HIV-1) infection and effectively suppresses HIV-1 replication to low or undetectable levels, corresponding with a recovery of CD4+ T cell counts.[1–3] ART treatment dramatically improves the survival rate of HIV-1-infected individuals and has transformed HIV-1 infection into a controllable illness. However, the need for lifelong therapy and difficulties in adherence to medication regimes are likely to lead to the emergence of drug-resistant HIV-1 strains. Long-term side effects, such as cardiovascular disease, hepatotoxicity and dementia, have been reported in association with HIV-1 infection.[4–6] The most serious deficiency of ART is that it cannot eradicate latent virus.[7] Once the treatment is interrupted, a replicable HIV-1 reemerges. Thus, the benefits of current ARTs are limited. Therefore, it remains necessary to discover and develop novel approaches for the management of HIV-1 infection, including treatment options used in combination with the ART.[8]

The report of the "Berlin Patient," who appears to have been cured of HIV-1 infection by stem cell transplantation with HIV-1 resistant CCR5Δ32/Δ32 cells[9] has had a major impact. This patient developed acute myelogenous leukemia and received bone marrow transplantation with cells bearing a homozygous Δ32 mutation in the CCR5 gene. No HIV-1 was detectable in this patient, even in the absence of ART.[10] However, allogeneic bone marrow transplantation as a cure for HIV-1 infection is not a realistic strategy because there is a risk of death, and the long-term effects are unclear. In contrast, gene therapy for HIV-1 has steadily progressed as an alternative to antiretroviral drug regimens.[11,12] A number of strategies have been developed, including strategies involving dominant negative inhibitory proteins, fusion inhibitors, antisense RNA, aptamers, RNA decoys, ribozymes, RNA interference, and HIV-1 entry inhibition.[13–18] These protocols target autologous T cells or hematopoietic stem cells for gene modification using retrovirus, lentivirus, or adenovirus vectors to deliver anti-HIV-1 payloads. Some of these methods have progressed to clinical trials.[19,20]

Recently, we proposed a new approach for gene therapy for HIV-1 using the endoribonuclease MazF.[21] MazF is encoded by *Escherichia coli* and specifically cleaves the ACA sequence of single-stranded RNAs. MazF does not interfere with ribosomal RNAs. When overexpressed in mammalian cells, MazF preferentially cleaves mRNA but not rRNA.[22] Previous studies have demonstrated that the expression of MazF under the control of the HIV-1 LTR promoter was successfully induced upon HIV-1 replication and rendered CD4+ T cells resistant to HIV-1 and simian/human immunodeficiency virus (SHIV) without affecting cellular mRNAs.[21,23] Because HIV-1 RNA has more than 240 ACA sequences, viral RNA is assumed to be highly susceptible to MazF. A key regulator of MazF expression in this system is the HIV-1 Tat protein, which activates transcription from the HIV-1 LTR.[24] In this system, the Tat protein induces HIV-1 replication and MazF expression. Furthermore, the autologous transplantation of MazF-modified CD4+ T cells in cynomolgus macaques has been shown to be safe, and the modified cells showed little or no immunogenicity.[25] These results suggest that the conditional expression of MazF is an attractive strategy for anti-HIV-1 gene therapy.

To investigate the safety, persistence and efficacy of MazF-modified CD4+ T cells in a nonhuman primate model *in vivo* in the presence of viral infection, six rhesus macaques were

[1]Center for Cell and Gene Therapy, Takara Bio Inc, Seta, Otsu, Shiga, Japan; [2]Tsukuba Primate Research Center, National Institute of Biomedical Innovation, Tsukuba, Ibaraki, Japan. Correspondence: Junichi Mineno, Center for Cell and Gene Therapy, Takara Bio Inc., Seta 3-4-1, Otsu, Shiga, 520–2193, Japan. E-mail: minenoj@takara-bio.co.jp or Hideto Chono, Center for Cell and Gene Therapy, Takara Bio Inc., Seta 3-4-1, Otsu, Shiga, 520–2193, Japan. E-mail: chonoh@takara-bio.co.jp

Keywords: gene therapy; HIV-1; MazF; primate model; rhesus macaque; retroviral vector; SHIV
Received 25 February 2014; accepted 27 April 2014; published online 10 June 2014. doi:10.1038/mtna.2014.20

infected with a SHIV 89.6P.[26] Four rhesus macaques were transplanted with MazF-modified CD4+ T (MazF-Tmac) cells, and two were transplanted with control ZsGreen1-modified CD4+ T (ZsG-Tmac) cells. After transplantation of the gene-modified cells, changes in the CD4+ T cell count values, changes in plasma SHIV viral loads, and the persistence of gene-modified cells were monitored throughout the experimental period. The humoral and cellular immune responses elicited by MazF were assessed. At necropsy, distributions of the transplanted MazF-Tmac cells in the distal lymphoid tissues, including several lymph nodes and the spleen, were analyzed.

Results

Study protocol and SHIV challenge

Six rhesus macaques (#12, #13, #14, #15, #16, and #17) were used for this experiment. Each rhesus macaque was challenged with SHIV 89.6P, followed by transplantation with autologous CD4+ T cells transduced with the MazF retroviral vector MT-MFR-PL2 (#12, #13, #14, and #15) or the control vector MT-ZGR-PL2 (#16 and #17) (Figure 1a). The rhesus macaques were monitored over 6 months for changes in CD4+ T cell counts, changes in SHIV viral loads in the plasma, persistence of the gene-modified cells, and the immune responses elicited by the gene-modified cells. An outline of the experiment is shown in Figure 1b,c. The dose of SHIV, day of infusion and experimental period are summarized in **Supplementary Table S1**. Initially, rhesus macaque #15 was challenged with (5000) 50% tissue culture infective dose ($TCID_{50}$), which we speculated would be a proper dose based on our previous experience; however, the viral loads declined to the limit of detection. We, therefore, increased the dose of $TCID_{50}$ for the other experiments. However, #12, #16, and #17 showed high viral loads, whereas #13 and #14 showed low viral loads. Such differences might have been due to individual variation in the sensitivity of the rhesus macaques used in this experiment.

Gene-modified T cell manufacturing and transplantation

MazF- or ZsGreen1-modified cells were manufactured from previously collected CD4+ T cells and transplanted into each rhesus macaque 2 months after SHIV 89.6P infection. Repeated transplantations were performed at 2-month intervals. To transplant more than 10^9 MazF-Tmac or ZsG-Tmac cells, $1–2\times10^7$ primary CD4+ T cells were recovered, stimulated, and transduced either with the MT-MFR-PL2 vector or the MT-ZGR-PL2 vector, and expanded as described in **Supplementary Materials and Methods**. The numbers and characteristics of the gene-modified CD4+ T cells for each transplantation are summarized in Table 1. The transduction efficiencies of the MazF and ZsGreen1 vectors were 52.0–69.5% and 53.8–75.7%, respectively. The gene-modified cells marked with a truncated form of the human low-affinity nerve growth factor receptor (LNGFR/CD271) were concentrated with an anti-CD271 monoclonal antibody for the first transplantation of rhesus macaques #12 and #14, and the second transplantation of rhesus macaques #13 and #15. The gene-modified cells that were positively selected were over 97% pure. There was no selection of control ZsG-Tmac cells for transplantation. The majority of the expanded cells were CD3+ CD4+ T cells

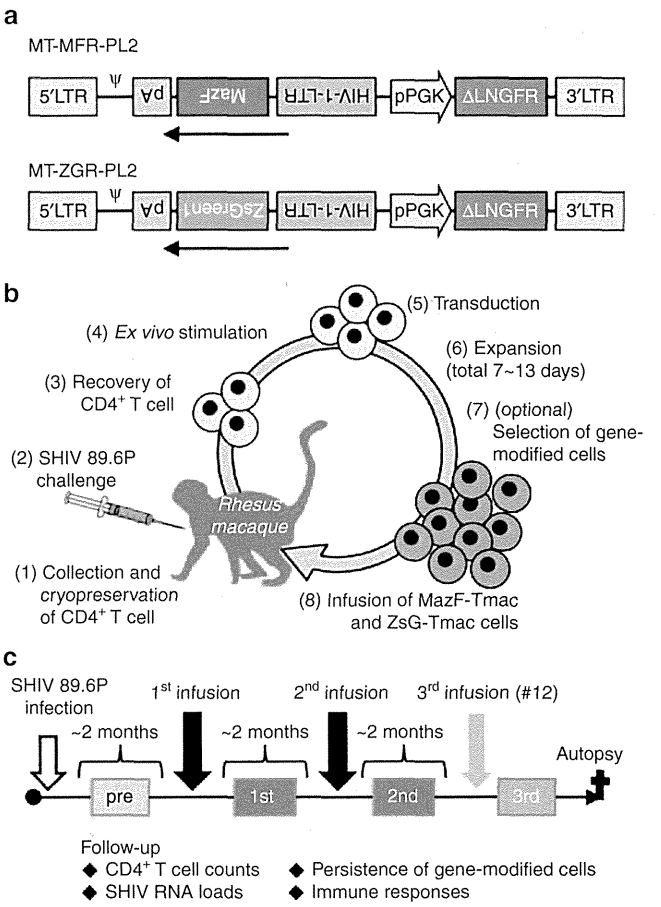

Figure 1 Diagram of autologous CD4+ T cell transplantation in a primate model. (a) Structures of the gamma-retroviral vectors MT-MFR-PL2 and MT-ZGR-PL2. LTR, long terminal repeat; MoMLV, Moloney murine leukemia virus; *LNGFR*, low-affinity nerve growth factor receptor gene; pPGK, phosphoglycerate kinase promoter. **(b)** *Flow diagram of gene therapy in the rhesus macaques.*[1] *Peripheral* blood was collected by apheresis; the CD4+ T cells were isolated and cryopreserved.[2] The rhesus macaques were challenged with SHIV 89.6P.[3,4] The CD4+ T cells were recovered and stimulated *ex vivo* with *anti-CD3/CD28 beads.*[5] *The stimulated cells were transduced twice* with retroviral vectors on days 3 and 4.[6] The transduced cells were expanded for an additional 3–9 days.[7] The ΔLNGFR-positive cells were selected at the second transplantation for rhesus macaques #13 and #15 and at the first transplantation for rhesus macaques #12 and #14.[8] On days 7–13, the expanded autologous cells were collected, washed and transplanted into the rhesus macaques intravenously. **(c)** Four rhesus macaques were transplanted with MazF-Tmac cells, and two were transplanted with control ZsG-Tmac cells. The rhesus macaques were followed over six months.

(>98%). More than 90% of these cells expressed CD95 and CD28, which are known markers of the central memory phenotype;[27] central memory cells generally have a longer lifespan than effector memory cells.[28] The expression levels of CXCR4, which is a known coreceptor for X4-tropic HIV-1 and SHIV entry, varied among animals and expansion periods.

Body weight and hematological data

There was no significant change in body weight throughout the experiment in the MazF-Tmac-transplanted rhesus macaques (see **Supplementary Figure S1a**). A gradual

Table 1 The summary of characteristics of gene-modified CD4+ T cells for each transplantation

	#12	#13	#14	#15	#16	#17
First transplantation						
Culture period (days)	13	9	13	9	9	9
Number of infused cells	2.1×10^9	3.0×10^9	2.3×10^9	1.6×10^9	1.6×10^9	1.1×10^9
CD271+ (gene-modified) (%)	97.2[a]	52.0	99.0[a]	54.1	53.8	75.0
CD3+ CD4+ (%)	98.3	99.9	99.0	99.8	99.2	99.8
CD28+ CD95+ CM (%)	93.4	97.5	95.4	98.7	N.D.	N.D.
CD28- CD95+ EM (%)	6.3	2.3	4.5	0.9	N.D.	N.D.
CXCR4+ (%)	36.3	63.2	8.9	65.5	67.9	52.6
Second transplantation						
Culture period (days)	9	13	9	13	10	10
Number of infused cells	2.7×10^9	3.3×10^9	1.8×10^9	2.7×10^9	3.8×10^9	2.8×10^9
Gene-modified (%)	69.5	96.3[a]	57.0	99.8[a]	55.2	75.7
CD3+ CD4+ (%)	99.0	99.9	98.7	99.8	99.5	99.6
CD28+ CD95+ CM (%)	96.9	90.8	97.7	97.6	N.D.	N.D.
CD28- CD95+ EM (%)	2.7	9.0	2.1	2.2	N.D.	N.D.
CXCR4+ (%)	55.4	47.8	35.7	84.0	63.5	63.4
Third transplantation						
Culture period (days)	7					
Number of infused cells	0.55×10^9					
Gene-modified (%)	65.4					
CD3+ CD4+ (%)	99.5					
CD28+ CD95+ CM (%)	96.9					
CD28- CD95+ EM (%)	3.1					
CXCR4+ (%)	77.0					

The autologous MazF-Tmac cells and the ZsG-Tmac cells were manufactured from the cryopreserved CD4+ T cells by stimulating the cells with anti-CD3/CD28 beads, and transducing them with the MT-MFR-PL2 and MT-ZGR-PL2 retroviral vectors. The CD3, CD4, CD28, CD95, CD271, and CXCR4 expression in the gene-modified cells at the time of transplantation were analyzed by flow cytometry.
[a]Gene-modified cells were concentrated based on their expression of the ΔLNGFR surface marker. CM, central memory; EM, effector memory; N.D., not determined.

decrease in body weight was observed in one ZsG-Tmac-transplanted rhesus macaque #16 by the end of the experiment (data not shown). Hematological data, including white blood cell count, hemoglobin concentration and platelets, were also analyzed, and significant changes were observed in rhesus macaque #16 at the end of the experiment (data not shown). Rhesus macaque #16 was sacrificed prior to the scheduled autopsy because of worsening symptoms. No significant changes were observed in any of the MazF-Tmac-transplanted rhesus macaques (see **Supplementary Figure S1b–d**). Thus, MazF-Tmac cells are considered safe based on the clinical observations.

CD4+ T cell counts in peripheral blood

To evaluate the impact of the autologous transplantation of gene-modified CD4+ T cells, the posttransplantation CD4+ T cell count values were compared with the values measured prior to transplantation. As shown in Figure 2a, the increases in the CD4+ T cell counts after transplantation of MazF-Tmac cells were significant in all four rhesus macaques, while no significant increases were observed in the two rhesus macaques transplanted with ZsG-Tmac cells. In the case of rhesus macaque #12, which was robustly infected with SHIV and had high viral loads (>10^5 copies/ml), the average CD4+ T cell count was 68 cells/μl before the gene therapy treatment, and increased to 107 cells/μl and 193 cells/μl after the first and second transplantation, respectively. Unfortunately, the mean CD4+ T cell count after the third transplantation decreased slightly to 139 cells/μl; this value was still higher than the baseline values.

The effectiveness was most clearly shown in the rhesus macaque #14, whose average CD4+ T cell count was 137 cells/μl before the gene therapy treatment, and subsequently increased to 329 cells/μl and 754 cells/μl after the first and second transplantations, respectively. To investigate the long-term safety of the treatment, this rhesus macaque was followed up for one and a half years. The other rhesus macaques (#13 and #15) had average CD4+ T cell counts of approximately 530 cells/μl before the gene therapy treatment that also increased to 1296 cells/μl and 856 cells/μl after the first transplantation, respectively, and retained these levels after the second transplantation. Thus, the transplantation of MazF-Tmac cells has the potential to increase CD4+ T cell counts.

Plasma SHIV viral loads

To investigate the influence of the transplantation of gene-modified cells, SHIV viral loads in the plasma were measured using quantitative PCR (qPCR). In rhesus macaque #15, the viral loads were below the detection limit at the time of gene therapy treatment. In rhesus macaques #13 and #14, the available data were limited to three time points due to a relatively short window in which they exhibited a stable set point before the infusion of MazF-Tmac cells. For this reason, we did not

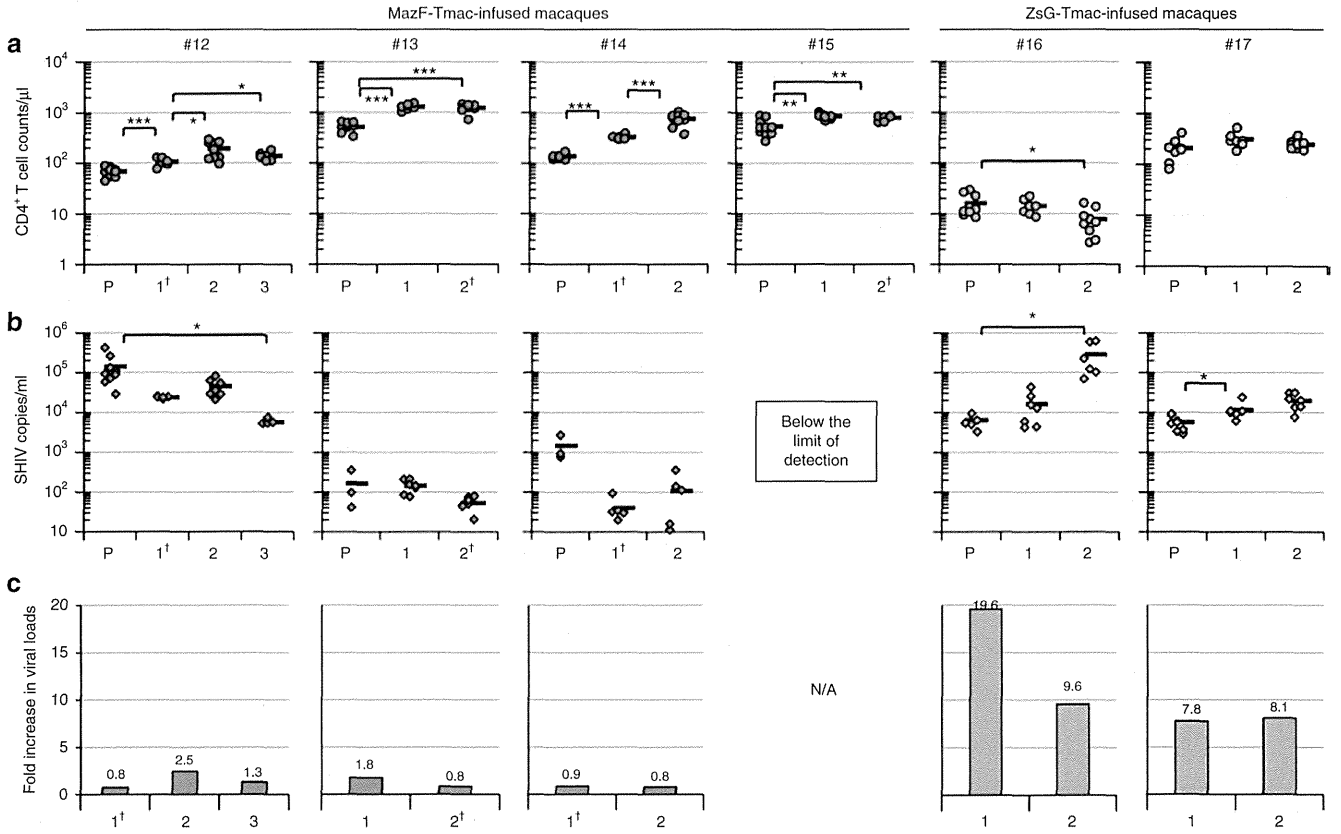

Figure 2 Changes in CD4⁺ T cell counts and viral loads. (a) The CD4⁺ T cell counts of MazF-Tmac- and ZsG-Tmac-transplanted rhesus macaques. The CD4⁺ T cell counts in the area of the viral load set point were averaged by multiple time point sampling 20 to 80 days after SHIV infection or transplantation. **(b)** Plasma SHIV viral RNA loads. The plasma SHIV viral RNA loads in the area of the set point were averaged by multiple time point sampling 20–80 days after SHIV infection or transplantation of gene-modified cells. **(c)** The fold increase of the plasma viral loads of MazF-Tmac- and ZsG-Tmac-transplanted rhesus macaques. The fold increase values were calculated by dividing [the average viral loads one week after transplantation of gene-modified cells] by [the average viral loads three weeks before transplantation of gene-modified cells]. P, pretransplantation of gene-modified cells; 1, after the first transplantation; 2, after the second transplantation; 3, after the third transplantation. Statistical significance indicated by Student's *t*-test (*$P < 0.05$; **$P < 0.01$; and ***$P < 0.001$). †Gene-modified cells were concentrated using the ΔLNGFR marker. N/A, not applicable due to undetectable viral loads.

employ statistical analyses between pre and postinfusion for these two macaques. However, there was no increase and tendency toward decrease in the viral loads after transplantation of MazF-Tmac cells (Figure 2b). For rhesus macaques #16 and #17, significant increases in the set point of SHIV viral loads were observed upon transplantation of ZsG-Tmac cells (Figure 2b). A dramatic rebound was detected immediately after transplantation (Figure 2c). These data indicate that the transplantation of ZsG-Tmac cells, which have no protective payload for SHIV, significantly impacted the viral loads. No remarkable rebound was observed after transplantation of MazF-Tmac cells (Figure 2c).

Longitudinal persistence of MazF-Tmac cells and ZsG-Tmac cells

To examine the *in vivo* persistence of transplanted MazF-Tmac cells and ZsG-Tmac cells, peripheral blood samples were collected to monitor the presence of gene-modified cells. The proviral copy number of the transduced retroviral vector was monitored by the qPCR method throughout the experiment. MazF-Tmac cells persisted for more than 6 months in the presence of SHIV. In particular, persistence for longer than one and a half years was observed in rhesus macaque #14. The ZsG-Tmac cells had nearly disappeared within two months after transplantation (Figure 3a). Similar results were obtained in flow cytometry analyses to detect the surface marker ΔLNGFR in the CD4⁺ T cells (Figure 3b). The calculated half-lives measured within 2 months of transplantation of the MazF-Tmac cells were much longer than that of the ZsG-Tmac cells (Table 2). The half-lives of the MazF-Tmac cells became even longer in the late phase of the experiment. Notably, in rhesus macaque #14, the half-life of the MazF-Tmac cells was 128.6 days when the period of analysis was extended to 9 months posttransplantation.

MazF antigen-specific interferon gamma (IFN-γ) enzyme-linked immunospot (ELISPOT) assay

To assess whether a cellular immune response was elicited by MazF-Tmac cells, an IFN-γ ELISPOT assay was performed. Peripheral blood mononuclear cells (PBMCs) from the MazF-Tmac-transplanted rhesus macaques were stimulated with a cocktail of MazF-overlapping peptides (see **Supplementary Figure S2**). As a negative control, PBMCs prepared from a normal (*i.e.*, untransplanted) rhesus

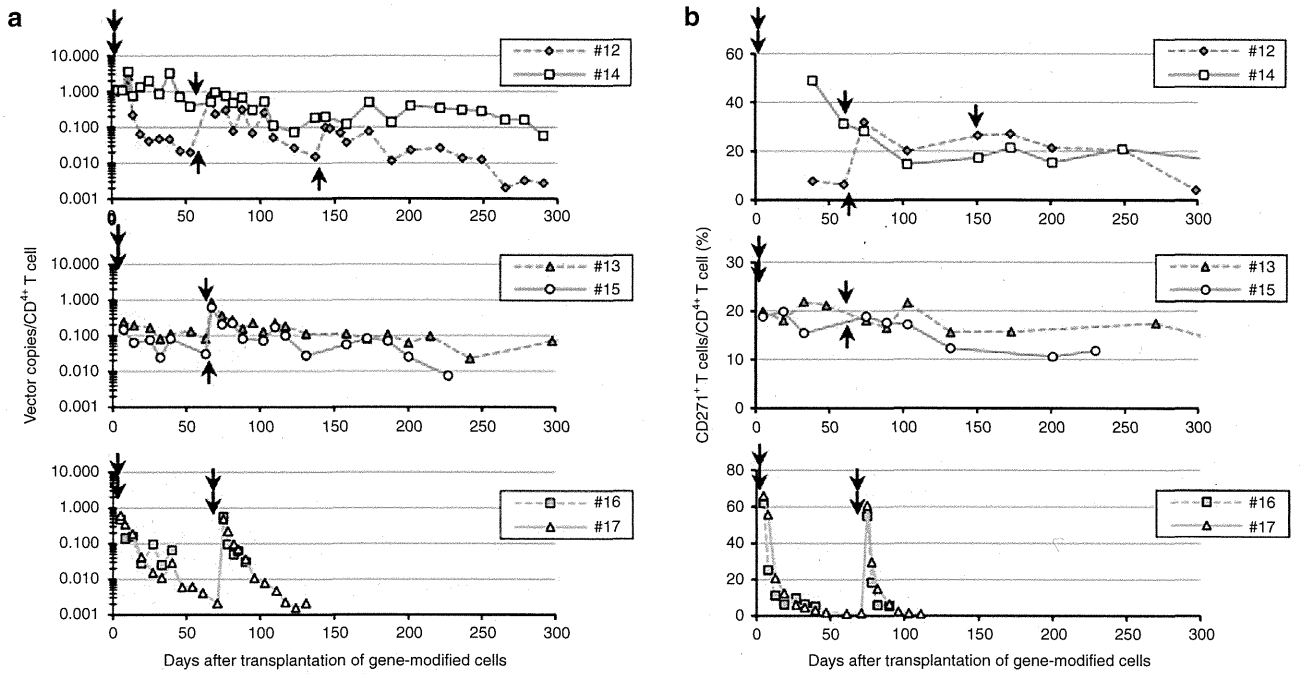

Figure 3 ***In vivo*** **persistence of MazF-Tmac and ZsG-Tmac cells. (a)** The persistence of MazF-Tmac cells and ZsG-Tmac cells was quantified using qPCR. The percentage of CD4+ T cells was analyzed using flow cytometry, and the proviral vector copy number was analyzed using qPCR. Using these data, the copy number of the transgene in CD4+ T cells was calculated. The arrows indicate the time point at which the gene-modified cells were transplanted. **(b)** The persistence of MazF-Tmac cells and ZsG-Tmac cells was quantified using flow cytometry. The percentage of gene-modified cells in the CD4+ T-cell population was determined after expanding the PBMCs with anti-CD3/CD28 beads stimulation for seven days, followed by antibody staining for CD4 and CD271 surface markers. The arrows indicate the time points at which the gene-modified cells were transplanted.

Table 2 The half-lives of gene-modified CD4+ T cells in each transplantation

	MazF-Tmac transplantation				ZsG-Tmac transplantation	
	#12	#13	#14	#15	#16	#17
First transplantation	7.7	42.8	35.6	32.4	3.9	4.6
Second transplantation	14.9	57.6	33.8	51.3	4.2	6.9
Third transplantation	29.0	N/A	N/A	N/A	N/A	N/A

The *in vivo* half-lives of the gene-modified cells in each rhesus macaque within a period of two months after transplantation was calculated by linear regression analyses using Microsoft Excel software.
N/A, not applicable.

macaque were stimulated. As shown in Figure 4a, no significant cellular immune responses related to the MazF-specific antigens were observed, indicating that the infused MazF-Tmac cells did not elicit a cellular immune response in the rhesus macaques in the presence of SHIV infection.

Detection of antibodies against MazF or ZsGreen1 in rhesus macaque blood

The evidence of longitudinal persistence of the MazF-Tmac cells supports the idea that these cells are not highly immunogenic; however, it is still important to assess the production of antibodies against MazF. As shown in Figure 4b, no significant production of antiMazF antibodies was detected in the blood samples from any of the rhesus macaques after transplantation with the MazF-Tmac cells. For the ZsG-Tmac cells, significant production of antibodies against ZsGreen1 was detected in rhesus macaque #17, while no antibody production was detected in rhesus macaque #16. The MazF-Tmac cells persisted for an extended period *in vivo*, and the MazF-Tmac-transplanted rhesus macaques produced no antibodies against MazF, indicating that the infused MazF-Tmac cells can be considered safe and not immunogenic in rhesus macaques in the presence of SHIV infection.

Distribution of gene-modified cells

At autopsy, lymphocytes isolated from several organs were analyzed for the distribution of the gene-modified cells using flow cytometry and qPCR. As shown in Table 3, ΔLNGFR-positive cells were detected by flow cytometry in the CD4+ T cells isolated from several lymph nodes, the spleen and the peripheral blood of the MazF-Tmac-transplanted rhesus macaques. A similar trend was observed in the qPCR analysis. The bone marrow, liver, and small intestine were also analyzed, but there were no detectable signs of gene-modified cells (data not shown). In the ZsG-Tmac-transplanted rhesus macaques, no gene-modified cells were detected in the organs or peripheral blood. These data strongly suggest that transplanted MazF-Tmac cells could circulate to the peripheral blood and the secondary lymphoid organs.

Histopathological analyses

It is advantageous to use primate models to investigate the safety of gene-modified cells because these animals can

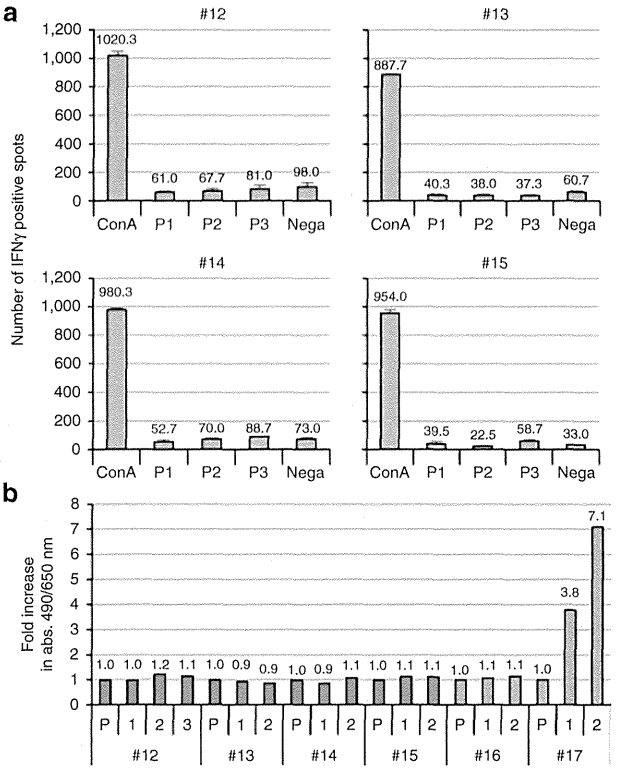

Figure 4 Detection of MazF-specific cellular and humoral immune responses. (a) IFN-γ enzyme-linked immunospot assay. The number of IFN-γ positive spots was measured under each stimulation condition. The PBMCs were prepared two months after the final MazF-Tmac cell transplantation. ConA: PBMCs from a MazF-Tmac-transplanted rhesus macaque were stimulated with concanavalin A. P1-3, PBMCs from a MazF-Tmac-transplanted rhesus macaque were stimulated with MazF peptide pools 1-3. Nega, nonstimulated PBMCs. Error bars represent the mean + SD. **(b)** Detection of MazF or ZsGreen1 specific humoral immune response using an enzyme-linked immunosorbent assay (ELISA). Plasma samples taken before transplantation (P), 4 weeks after the first transplantation,(1) 4 weeks after the second transplantation,(2) and 4 weeks after the third transplantation(3) of gene-modified cells were tested for the presence of antibodies against MazF in rhesus macaques #12, #13, #14, and #15 and for ZsGreen1 rhesus macaques #16 and #17. The relative fold increases in the absorbance values compared with the pretransplantation values are shown.

be used for surgical pathological analyses. We performed experimental autopsies at the end of the experiment. The histopathological findings of the specimens are summarized in **Supplementary Table S2**. Severe involution of the thymus was observed in rhesus macaque #12. This involution appeared to be the result of a physiological factor, such as aging, and was considered to be unrelated to the treatment of transplantation of MazF-Tmac cells. No serious adverse events related to MazF-Tmac cell transplantation were observed in any of the rhesus macaques in this treatment group.

Rhesus macaques #16 and #17 were affected by SHIV infection or transplantation of ZsG-Tmac cells, which have no SHIV resistance payload. As shown in **Supplementary Figure S3**, several disorders were observed in the axillary lymph nodes of the ZsG-Tmac-transplanted macaques,

Table 3 Distribution of gene-modified cells in lymphoid tissues

	MazF-Tmac transplantation							
	#12		#13		#14		#15	
	FCM (%)[a]	qPCR[b]	FCM (%)[a]	qPCR[b]	FCM (%)[a]	qPCR[b]	FCM (%)[a]	qPCR[b]
PBMC	4.1	2.9	15.4	18.0	4.8	11.1	11.8	26.4
Inguinal LN	N/A	3.0	13.2	16.8	4.2	8.1	7.3	17.1
Axillary LN	N/A	3.1	11.9	17.7	2.7	6.5	6.7	17.3
Mesenteric LN	N/A	0.54	13.0	18.2	4.0	10.1	5.6	14.3
Spleen	N/A	0.28	13.3	7.4	2.7	3.9	7.2	14.7

The lymphocytes isolated from several organs at autopsy were analyzed by flow cytometry and qPCR to determine the distribution of gene-modified cells.
FCM, flow cytometry; LN, lymph nodes; N/A, not applicable; PBMC, peripheral blood mononuclear cell.
[a]The percentage of ΔLNGFR-positive CD4+ T cells was determined by flow cytometry. qPCR. [b]Proviral vector copy numbers per 10^2 CD4+ T cells.

including a decrease in size, destruction of the structures, (see **Supplementary Figure S3a**) and a decrease in lymphoid cells (see **Supplementary Figure S3b**). These disorders were not observed in the MazF-Tmac-transplanted rhesus macaques. Rhesus macaque #16 was seriously affected by atrophy of the thymus, a decrease in lymphocytes in the inguinal and mesenteric lymph nodes, atrophy and lymphoid necrosis in the splenic marginal zone and a decrease in lymphoid cells in the periarterial lymphatic sheath and red pulp (see **Supplementary Table S2**). These observations were considered to be representative of changes relevant to the SHIV infection or transplantation of ZsG-Tmac cells. In rhesus macaque #17, atrophy of the thymus and a decrease in the lymphocytes in the inguinal lymph nodes were considered to be related to SHIV infection or the transplantation of ZsG-Tmac cells.

Function of persisting MazF-Tmac cells

To examine the Tat-dependent expression of MazF and its antiviral efficacy maintained in the rhesus macaques, CD4+ T cells were isolated from the peripheral blood at 5 and 18 months after the first transplantation in rhesus macaques #13 and #15 and rhesus macaque #14, respectively. The expression of the MazF protein, the proviral copy numbers of SHIV and the production of SHIV in *ex vivo* culture were analyzed (Figure 5a).

A qPCR assay and Western blotting analysis were employed in PBMCs and isolated CD4+ T cell samples from rhesus macaques #13 and #15 to detect the intact expression of MazF *in vivo*; however, there was no signal with either method. We speculate that the specific detection of MazF expression *in vivo* is challenging due to a limited number of MazF-Tmac cells in PBMCs and the low infectivity of SHIV *in vivo* compared with *in vitro* conditions. Next, the isolated CD4+ T cells were expanded *ex vivo* for seven days, during which SHIV actively replicated, and Tat-dependent expression was expected to be induced in the MazF-Tmac cells in the CD4+ T-cell population. The expression of MazF was observed in the expanded cells by Western blotting analysis (Figure 5b). Although the intact expression of MazF *in vivo* was below the detection limit by qPCR and Western blotting, the Tat-dependent conditional expression system was maintained long term after transplantation.

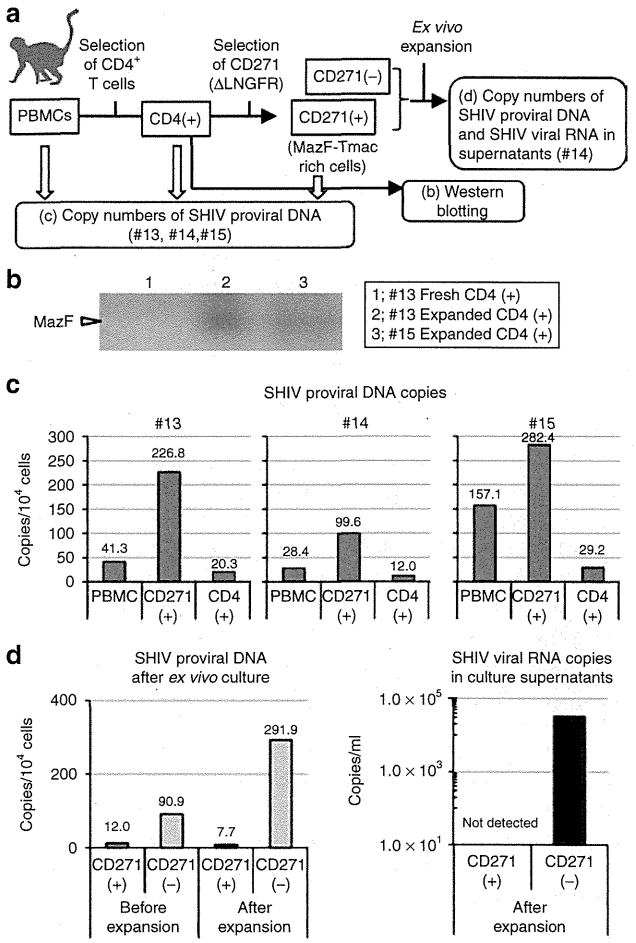

Figure 5 Function of long-term persisting MazF-Tmac cells. **(a)** Outline of the experiment. **(b)** CD4+ T cells were isolated from the peripheral blood of MazF-Tmac-transplanted rhesus macaques five months after the first transplantation. The isolated CD4+ T cells were expanded for seven days *ex vivo* and used for Western blotting analysis to detect the expression of MazF. **(c)** The CD271-positive and -negative cells were separated from the isolated CD4+ T cells of rhesus macaques #13, #14, and #15. DNA samples were collected from the PBMCs, the CD4+ T cells and the CD271+-MazF-Tmac-enriched population to analyze the proviral copy number of SHIV. **(d)** The CD271+-MazF-Tmac-enriched and CD271−-MazF-Tmac-negative populations isolated from rhesus macaque #14 were expanded *ex vivo* for 7 days. Changes in the SHIV proviral DNA levels in the cells and the SHIV RNA levels in the supernatants were analyzed in the CD271+-MazF-Tmac-enriched and CD271−MazF–Tmac-negative populations.

The persisted MazF-Tmac cells, which expressed the surface marker ΔLNGFR, were concentrated from a blood sample taken from rhesus macaques #13, #14, and #15 using an anti-CD271 monoclonal antibody. The number of proviral DNA copies of SHIV was measured in the PBMC population, CD4+ T-cell population and CD271+-MazF-Tmac-enriched population. As shown in Figure 5c, the number of proviral SHIV copies in the CD271+-MazF-Tmac-enriched population was one log lower than that in the CD4+ T-cell population in all three MazF-Tmac-transplanted rhesus macaques. To assess the function of the MazF-Tmac cells after transplantation, the CD271+-MazF-Tmac-enriched population and CD271−-MazF-Tmac-negative population isolated from rhesus macaque #14 at 18 months after transplantation were expanded *ex vivo* for 7 days in the absence of antiviral drugs. Changes in the SHIV proviral DNA level in the cells and the SHIV RNA level in the supernatants were analyzed. As shown in Figure 5d, the SHIV proviral DNA of the CD271−-MazF-Tmac-negative population increased by more than threefold after the expansion, indicating that SHIV was replicated in the CD271−-MazF-Tmac-negative population. The SHIV proviral DNA of the CD271+-MazF-Tmac-enriched population decreased slightly, indicating that replication of SHIV *ex vivo* was suppressed in the CD271+-MazF-Tmac-enriched population. The SHIV RNA copies accumulated in the supernatant of the CD271−-MazF-T-negative population in the absence of antiviral drugs, while there were no detectable SHIV RNA copies in the culture supernatants of the CD271+-MazF-Tmac-enriched population. These data indicate that the MazF-Tmac cells (CD271+ cells) are functional and possess the capability to suppress SHIV replication even one and a half years after transplantation.

Discussion

MazF is an endoribonuclease that specifically cleaves ACA sequences in RNA.[29] Because there are more than 240 ACA sequences in HIV-1 RNA, HIV-1 should have almost no chance to gain a MazF-related escape mutation. Therefore, anti-HIV-1 gene therapy using MazF is an attractive strategy to suppress a broad spectrum of HIV-1. HIV-1 Tat-dependent conditional expression of MazF in CD4+ T cells suppresses the replication of HIV-1 and SHIV 89.6P without affecting cellular mRNAs.[21,23] Because MazF is a bacterial protein and has never been tested in humans, it is important to assess the safety of the MazF-system *in vivo* using a nonhuman primate model. In a previous report, we showed the long-term persistence and safety of autologous transplantation of MazF-Tmac cells using cynomolgus macaques[25] that were not infected with a pathogenic virus. To obtain a better understanding of the MazF-modified CD4+ T cells in the presence of a viral infection *in vivo*, rhesus macaques were infected with pathogenic SHIV 89.6P and transplanted with autologous MazF-Tmac cells.

An engraftment of 1–2% of gene-modified cells in the peripheral circulation has been reported after the transplantation of approximately 10^{10} cells in adoptive T cell transfer gene therapy for humans,[13] and higher cell doses result in higher measurable engraftment levels.[30] We decided to transplant more than 10^9 cells in the primate model, reflecting one-tenth of the scale of the human gene therapy trials. To investigate the influence of repeated transplantations, transplantations were performed two or three times in this study.

The CD4+ T cell count values of the SHIV-infected rhesus macaques increased after the transplantation of the MazF-Tmac cells with statistical significance, while such increases were not observed in the ZsG-Tmac-transplanted rhesus macaques. The infused MazF-Tmac cells persisted for a long period *in vivo*, with half-lives ranging between 7.7 and 58 days. It is also possible that some of the MazF-Tmac cells were vigorously infected by SHIV and killed. To gain a longer

therapeutic benefit from the infusion of gene-modified T cells, gene-modified T cells are expected to expand *in vivo*; however, MazF-Tmac cells did not preferentially expand *in vivo* in this experiment. We are currently addressing this issue and attempting to confer self-expansion capability on MazF-Tmac cells in the presence of viral infections.

The viral load of MazF-Tmac-infused macaques did not decrease dramatically. In general, the major roles of CD4+ helper T cell are activation and regulation of the immune system. The helper T cell does not directly affect the viral load or infected cells as like cytotoxic T-lymphocytes or antibodies, so we speculate that the dramatic decrease of SHIV viral load was not observed though CD4+ T cell counts increased.

We used six rhesus macaques, which were divided in two arms—four rhesus macaques for MazF-modified T cell-treated arm and two macaques for ZsGreen1-modified T cell-treated arm. Only one rhesus macaque in the MazF-modified T cell-treated arm was highly infected with SHIV; the other three were weakly infected. However, SHIV proviral DNA was detected in the PBMCs of all of the macaques, and SHIV reproduced in culture medium when collected PBMCs were expanded *ex vivo* (Figure 5). The primary purpose of this experiment was to confirm the safety and persistence of MazF-Tmac cells in the presence of SHIV infection; thus, we used not only high viral load macaque but also weakly infected macaques for this study. No immune responses related to MazF were observed, and half-lives were extended after the repeated transplantation. The evidence of longitudinal persistence of MazF-Tmac cells suggests that MazF-modified T cells are not highly immunogenic. Because MazF remains at a constant low level upon viral infection,[23] MazF-Tmac cells are unlikely to activate an immune response. To obtain more safety information on MazF-modified CD4+ T cells in the presence of HIV infection, further investigations are needed, and a clinical trial entitled "A phase I, open label, dual cohort, single center study to evaluate the safety, tolerability and immunogenicity of autologous CD4 T cells modified with a retroviral vector expressing the *mazF* endoribonuclease gene in patients with HIV" is now ongoing in the United States (clinicaltrials.gov, identifier NCT01787994). Antiviral effect would also be assessed in the cohort 2 arm of this clinical trial.

In contrast, the infused ZsG-Tmac cells did not persist for an extended period *in vivo*, and the half-lives were not extended after repeated transplantation. The transient rebound of SHIV and marked decrease in the number of vector copies occurred simultaneously within 2 weeks after the transplantation of ZsG-Tmac cells; antiZsGreen1 antibodies developed gradually and reached their maximum level 40 days after the transplantation (see **Supplementary Figure S4**). We hypothesize that the ZsG-Tmac cells, which have no payload related to SHIV resistance, secreted a large amount of SHIV particles after infection and were destroyed by SHIV *in vivo*. The internalization of ZsGreen1 protein and antigen presentation by antigen-presenting cells induced the immune responses. In the case of rhesus macaque #17, ZsGreen1 protein might have been highly expressed by vigorous infection and triggered antibody production. In the case of rhesus macaque #16, ZsGreen1 protein was most likely expressed abundantly as in #17. Because this rhesus macaque exhibited severely reduced CD4+ T cell counts, we speculate that the B cells were not stimulated by Th2 effector cells due to a lack of CD4+ helper T cells; thus, no antibodies against ZsGreen1 were detected in rhesus macaque #16.

To address whether MazF-modified CD4+ T cells are associated with carcinogenicity *in vivo,* clonal expansion of the gene-modified cells was assessed using the linear amplification-mediated-PCR (LAM-PCR) method,[31] which traces the progeny of transduced cells by detecting the random insertion of the retrovirus or lentivirus vector. Although the preliminary data were collected from four macaques during a limited experimental period, there were no specific clonal expansions in any of the MazF-Tmac-transplanted rhesus macaques (see **Supplementary Figure S5**).

The histopathological analyses of the major organs, as well as the secondary lymphoid tissues, revealed that the transplantation of the MazF-Tmac cells was not associated with any carcinogenicity during the study period (see **Supplementary Figure S3** and **Supplementary Table S2**). A decrease in lymphocyte number was observed in the inguinal and axillary lymph nodes of the ZsG-Tmac-transplanted rhesus macaques (see **Supplementary Figure S3** and **Supplementary Table S2**). Although the transplanted ZsG-Tmac cells were not detected at the time of autopsy, the ZsG-Tmac cells might have migrated to the lymph nodes after transplantation, and the SHIV might have vigorously replicated in the migrated ZsG-Tmac cells, leading to cell death and, ultimately, bystander apoptosis of the neighboring uninfected cells and damage to the lymph nodes.[32] There was no such damage to the lymph nodes in rhesus macaque #12, which exhibited the highest SHIV viral loads and had undergone transplantation of MazF-Tmac cells three times.

Because gene therapy for HIV-1 should aim to reconstitute an HIV-1-resistant immune system, it is important for the gene-modified cells to not only inhibit viral replication but also maintain their distribution for long periods *in vivo*. Although the long-term persistence of gene-modified T cells or hematopoietic stem cells has been reported in the context of human gene therapy, it is difficult to obtain information about the distribution of these cells throughout the body. The use of primate models is advantageous for investigating the distribution pattern. At the time of the experimental autopsy, lymphocytes were isolated from the principal organs. MazF-Tmac cells were detected in the secondary lymphoid tissues, including several lymph nodes and the spleen, as well as the peripheral blood. A similar tendency was observed in previous data from cynomolgus macaques.[25] In contrast, ZsG-Tmac cells were not detected in any of the organs at the time of autopsy. The MazF-Tmac cells tend to persist primarily in the peripheral blood and secondary lymphoid tissues, regardless of the SHIV infection status.

The number of proviral SHIV DNA copies in the harvested CD271+-MazF-Tmac-enriched population was significantly lower than that in the CD4+ T-cell population (Figure 5c). The exact mechanism of low SHIV copies in MazF-Tmac cells *in vivo* remains unclear. We examined the expression of coreceptor CXCR4 in gene-modified cells at the time of infusion, and no difference in expression levels was observed between the gene-modified and unmodified cells. One possible hypothesis is that the majority of the SHIV-infected CD4+

T cells were infected at the acute infection stage but that the infused cells are less infected during chronic infection stage. Alternatively, leaky expression of MazF in the infused MazF-Tmac cells may inhibit the integration of SHIV. Another possibility is that vigorously infected MazF-Tmac cells died off after the over-induction of MazF expression. Further investigation is needed to reveal the mechanism.

We analyzed the function of the MazF-Tmac cells that persisted long after transplantation. Conditional MazF expression system was maintained and MazF protein expressed in T cells harvested from the rhesus macaques long after transplantation. In the freshly isolated samples, which are not expanded *ex vivo*, MazF signal was beyond detection (Figure 5b, lane 1). This phenomenon was considered due to low frequency of SHIV infection in MazF-Tmac cells (Figure 5c). However, we believe that low sensitivity to SHIV and low expression of MazF may contribute to the stable long-term persistence of MazF-Tmac cells, even in the presence of SHIV. Moreover, our qPCR analysis demonstrated that SHIV replication was blocked (Figure 5d). Although these data are from only one macaque, it appears that the MazF expression system was maintained, and the expressed MazF was functional long after transplantation.

Transplantation with MazF-Tmac cells contributed to an increase in the CD4$^+$ T cell counts, and the MazF-Tmac cells showed little or no immunogenicity in rhesus macaques in the presence of SHIV infection, suggesting that the autologous transplantation of MazF-modified CD4$^+$ T cells is an attractive strategy for HIV-1 gene therapy.

Materials and methods

General laboratory statement. Research sample processing and freezing were performed in a biosafety level (BSL) 3 laboratory at the Tsukuba Primate Research Center in the National Institute of Biomedical Innovation (NIBIO, Ibaraki, Japan). Laboratory analyses were performed in BSL2 laboratories at the Tsukuba Primate Research Center in NIBIO and at the Center for Cell and Gene Therapy of Takara Bio, which uses established standard operating procedures and protocols for sample processing, freezing, and analysis.

Study design. The animal study protocol was approved by the Ministry of Education, Culture, Sports, Science and Technology of Japan (identifier 20–8156), and by the Animal Welfare and Animal Care Committee of the NIBIO (identifier DS20-98R3). The study was conducted according to the "Rules for Animal Care and the Guiding Principles for Animal Experiments Using Nonhuman Primates" formulated by the Primate Society of Japan,[33] and in accordance with the recommendations of the Weatherall report, "The use of nonhuman primates in research" and the "Rules for Animal Care and Management of the Tsukuba Primate Research Center."[34] The experimental design is diagrammed in Figure 1. Six rhesus macaques, #12, #13, #14, #15, #16, and #17, were used for this experiment. CD4$^+$ T cells were isolated from the blood samples taken from each rhesus macaque before the challenge with SHIV and cryopreserved as described below. After confirming the set point of the SHIV viral loads, the gene-modified CD4$^+$ T cells were manufactured and transplanted as described in **Supplementary Materials**. Autologous CD4$^+$ T cells were transduced with the MazF retroviral vector MT-MFR-PL2 (#12, #13, #14, and #15) or the control vector MT-ZGR-PL2 (#16 and #17).

Animals. The Burmese rhesus macaques were maintained at the Tsukuba Primate Research Center in NIBIO. All surgical and invasive clinical procedures were conducted in a surgical facility using aseptic techniques and comprehensive physiologic monitoring. Ketamine hydrochloride (Ketalar, 10 mg/kg; Daiichi-Sankyo, Tokyo, Japan) was used to induce anesthesia for all clinical procedures associated with the study protocol, including blood sampling, gene-modified cell administration and clinical examinations or treatment.

SHIV 89.6P virus. A CXCR4-tropic SHIV 89.6P[26] was used for this experiment. SHIV 89.6P was propagated in rhesus macaque PBMCs. The culture supernatants were harvested, and the 50% tissue culture infective dose ($TCID_{50}$) was determined by infecting the CD4$^+$ human T-lymphoblastoid cell line M8166 with dilutions of the virus.[35] All the stock viruses were stored at –80°C until use. An intravenous challenge with SHIV 89.6P was performed at 5.0×10^3–1.8×10^5 $TCID_{50}$ (**Supplementary Table S1**).

Gibbon ape leukemia virus (GaLV)-enveloped gamma-retroviral vector MT-MFR-PL2 and MT-ZGR-PL2. The preparation of the retroviral vector used in this study has been previously described.[21] Briefly, an HIV-1-LTR-MazF-polyA cassette was introduced in the direction opposite of the MoMLV-LTR at the multiple cloning site of the retroviral vector plasmid pMT.[36] The Δ*LNGFR* gene[37] was introduced into the retrovirus vector as a surface marker. The Δ*LNGFR* gene is under the control of the human phosphoglycerate kinase (PGK) promoter. The resultant MT-MFR-PL2 was introduced into the packaging cell line PG13 (ATCC CRL-10686) and the GaLV-enveloped gamma-retroviral vector MT-MFR-PL2 was obtained by harvesting the culture fluid of the producer cells. For the control experiment, the *mazF* gene was replaced with the gene encoding the fluorescent ZsGreen1 protein (MT-ZGR-PL2). The GaLV-enveloped MT-ZGR-PL2 was obtained by harvesting the culture fluid of the PG13 derived producer cells.

CD4$^+$ T cells. Prior to the challenge with SHIV 89.6P, the peripheral blood of rhesus macaques was collected by apheresis as described previously.[38] The CD4$^+$ T cells were positively isolated using anti-CD4 antibody conjugated magnetic beads (Dynal CD4 Positive Isolation Kit, Life Technologies, Carlsbad, CA) according to the manufacturer's instructions. The isolated CD4$^+$ T cells were cryopreserved and stored at –80°C until use.

Manufacturing autologous gene-modified CD4$^+$ T cells and transplantation into rhesus macaques. Refer to the **Supplementary Materials**.

Measurement of hematological data. Refer to the **Supplementary Materials.**

Flow cytometry analyses. Refer to the **Supplementary Materials.**

Quantification of gene-modified CD4+ T cells. Refer to the **Supplementary Materials.**

Analyses of the SHIV viral loads in plasma. Refer to the **Supplementary Materials.**

Detection of MazF antigen-specific IFN-γ secreting cells. Refer to the **Supplementary Materials.**

Detection of anti-MazF or anti-ZsGreen1 antibodies in rhesus macaque blood. Refer to the **Supplementary Materials.**

Collection of lymphocytes from several organs. Refer to the **Supplementary Materials.**

Examination of function and antiviral efficacy of persisting MazF-Tmac cells. Refer to the **Supplementary Materials.**

LAM-PCR. Refer to the **Supplementary Materials.**

Western blotting. Refer to the **Supplementary Materials.**

Supplementary material

Figure S1. Body weight and hematological data.
Figure S2. MazF peptides used for the IFN-γ enzyme-linked immunospot assay.
Figure S3. Histopathological analysis of axillary lymph nodes.
Figure S4. Changes in SHIV viral loads, ZsGreen1 proviral copy numbers and production of anti-ZsGreen1 antibodies of rhesus macaque #17.
Figure S5. Linear amplification-mediated (LAM)-PCR.
Table S1. Dose of SHIV 89.6P TCID50 used to infect each rhesus macaque and the time of transplantation of the gene-modified cells.
Table S2. Analysis of the in vivo safety (individual histopathological findings from the autopsy samples).
Materials and methods

Acknowledgments. The authors thank the staff of the Tsukuba Primate Research Center and Corporation for Production and Research of Laboratory Primates for their kind care and expert handling of the animals. The authors thank Keith A. Reimann of Harvard Medical School and Tomoyuki Miura of Kyoto University for providing the SHIV 89.6P. The authors thank the members of the Center for Cell and Gene Therapy of Takara Bio Inc., Koichi Inoue and Katsuyuki Dodo for their contributions and helpful advice, and Hiroshi Tsuda, Tomomi Sakuraba, and Mayumi Shimomura for technical support. The authors have no support or funding to report. The animal study was designed by Hideto Chono, Naoki Saito, Hiroaki Shibata, Naohide Ageyama, Yasuhiro Yasutomi and Junichi Mineno. Gene-modified T cells were manufactured by Naoki Saito and Hideto Chono. All surgical and invasive clinical procedures were conducted under the supervision of Naohide Ageyama. Blood samples were prepared by Hiroaki Shibata. The laboratory analyses were performed by Naoki Saito. The manuscript was written by Hideto Chono and Naoki Saito. All authors discussed and interpreted results. Naoki Saito, Hideto Chono and Junichi Mineno are employees of Takara Bio Inc. (http://www.takara-bio.com). European patent applications EP1921136B1 "Nucleic acid for treatment or prevention of immunodeficiency virus infection" and EP2138580B1 "Vector for gene therapy" were filed through Takara Bio Inc. These interests do not alter the authors' adherence to the Journal's policies regarding sharing data and materials. The other authors declared that they have no competing interests.

1. Kitahata, MM, Gange, SJ, Abraham, AG, Merriman, B, Saag, MS, Justice, AC *et al.* (2009). Effect of early versus deferred antiretroviral therapy for HIV on survival. *N Engl J Med* **360**: 1815–1826.
2. Maartens, G and Boulle, A (2007). CD4 T-cell responses to combination antiretroviral therapy. *Lancet* **370**: 366–368.
3. Geng, EH and Deeks, SG (2009). CD4+ T cell recovery with antiretroviral therapy: more than the sum of the parts. *Clin Infect Dis* **48**: 362–364.
4. Lekakis, J and Ikonomidis, I (2010). Cardiovascular complications of AIDS. *Curr Opin Crit Care* **16**: 408–412.
5. Núñez, M (2010). Clinical syndromes and consequences of antiretroviral-related hepatotoxicity. *Hepatology* **52**: 1143–1155.
6. Cheung, MC, Pantanowitz, L and Dezube, BJ (2005). AIDS-related malignancies: emerging challenges in the era of highly active antiretroviral therapy. *Oncologist* **10**: 412–426.
7. Siliciano, RF and Greene, WC (2011). HIV latency. *Cold Spring Harb Perspect Med* **1**: a007096.
8. Richman, DD, Margolis, DM, Delaney, M, Greene, WC, Hazuda, D and Pomerantz, RJ (2009). The challenge of finding a cure for HIV infection. *Science* **323**: 1304–1307.
9. Hütter, G, Nowak, D, Mossner, M, Ganepola, S, Müssig, A, Allers, K *et al.* (2009). Long-term control of HIV by CCR5 Delta32/Delta32 stem-cell transplantation. *N Engl J Med* **360**: 692–698.
10. Allers, K, Hutter, G, Hofmann, J, Loddenkemper, C, Rieger, K, Thiel, E *et al.* (2011). Evidence for the cure of HIV infection by CCR5Delta32/Delta32 stem cell transplantation. *Blood* **117**: 2791–2799.
11. Sarver, N and Rossi, J (1993). Gene therapy: a bold direction for HIV-1 treatment. *AIDS Res Hum Retroviruses* **9**: 483–487.
12. Dropulić, B and Jeang, KT (1994). Gene therapy for human immunodeficiency virus infection: genetic antiviral strategies and targets for intervention. *Hum Gene Ther* **5**: 927–939.
13. Levine, BL, Humeau, LM, Boyer, J, MacGregor, RR, Rebello, T, Lu, X *et al.* (2006). Gene transfer in humans using a conditionally replicating lentiviral vector. *Proc Natl Acad Sci USA* **103**: 17372–17377.
14. Morris, KV and Rossi, JJ (2006). Lentivirus-mediated RNA interference therapy for human immunodeficiency virus type 1 infection. *Hum Gene Ther* **17**: 479–486.
15. Rossi, JJ, June, CH and Kohn, DB (2007). Genetic therapies against HIV. *Nat Biotechnol* **25**: 1444–1454.
16. van Lunzen, J, Glaunsinger, T, Stahmer, I, von Baehr, V, Baum, C, Schilz, A *et al.* (2007). Transfer of autologous gene-modified T cells in HIV-infected patients with advanced immunodeficiency and drug-resistant virus. *Mol Ther* **15**: 1024–1033.
17. Li, MJ, Kim, J, Li, S, Zaia, J, Yee, JK, Anderson, J *et al.* (2005). Long-term inhibition of HIV-1 infection in primary hematopoietic cells by lentiviral vector delivery of a triple combination of anti-HIV shRNA, anti-CCR5 ribozyme, and a nucleolar-localizing TAR decoy. *Mol Ther* **12**: 900–909.
18. Hoxie, JA and June, CH (2012). Novel cell and gene therapies for HIV. *Cold Spring Harb Perspect Med* **2**: a007179.
19. Cannon, P and June, C (2011). Chemokine receptor 5 knockout strategies. *Curr Opin HIV AIDS* **6**: 74–79.
20. Tebas, P, Stein, D, Binder-Scholl, G, Mukherjee, R, Brady, T, Rebello, T *et al.* (2013). Antiviral effects of autologous CD4 T cells genetically modified with a conditionally replicating lentiviral vector expressing long antisense to HIV. *Blood* **121**: 1524–1533.
21. Chono, H, Matsumoto, K, Tsuda, H, Saito, N, Lee, K, Kim, S *et al.* (2011). Acquisition of HIV-1 resistance in T lymphocytes using an ACA-specific E. coli mRNA interferase. *Hum Gene Ther* **22**: 35–43.
22. Shimazu, T, Degenhardt, K, Nur-E-Kamal, A, Zhang, J, Yoshida, T, Zhang, Y *et al.* (2007). NBK/BIK antagonizes MCL-1 and BCL-XL and activates BAK-mediated apoptosis in response to protein synthesis inhibition. *Genes Dev* **21**: 929–941.
23. Okamoto, M, Chono, H, Kawano, Y, Saito, N, Tsuda, H, Inoue, K *et al.* (2013). Sustained inhibition of HIV-1 replication by conditional expression of the *E. coli*-derived endoribonuclease MazF in CD4+ T cells. *Hum Gene Ther Methods* **24**: 94–103.

24. Berkhout, B, Silverman, RH and Jeang, KT (1989). Tat trans-activates the human immunodeficiency virus through a nascent RNA target. *Cell* **59**: 273–282.
25. Chono, H, Saito, N, Tsuda, H, Shibata, H, Ageyama, N, Terao, K *et al.* (2011). *In vivo* safety and persistence of endoribonuclease gene-transduced CD4+ T cells in cynomolgus macaques for HIV-1 gene therapy model. *PLoS One* **6**: e23585.
26. Reimann, KA, Li, JT, Voss, G, Lekutis, C, Tenner-Racz, K, Racz, P *et al.* (1996). An env gene derived from a primary human immunodeficiency virus type 1 isolate confers high *in vivo* replicative capacity to a chimeric simian/human immunodeficiency virus in rhesus monkeys. *J Virol* **70**: 3198–3206.
27. Pitcher, CJ, Hagen, SI, Walker, JM, Lum, R, Mitchell, BL, Maino, VC *et al.* (2002). Development and homeostasis of T cell memory in rhesus macaque. *J Immunol* **168**: 29–43.
28. Klebanoff, CA, Gattinoni, L, Torabi-Parizi, P, Kerstann, K, Cardones, AR, Finkelstein, SE *et al.* (2005). Central memory self/tumor-reactive CD8+ T cells confer superior antitumor immunity compared with effector memory T cells. *Proc Natl Acad Sci USA* **102**: 9571–9576.
29. Zhang, Y, Zhang, J, Hoeflich, KP, Ikura, M, Qing, G and Inouye, M (2003). MazF cleaves cellular mRNAs specifically at ACA to block protein synthesis in *Escherichia coli*. *Mol Cell* **12**: 913–923.
30. Ranga, U, Woffendin, C, Verma, S, Xu, L, June, CH, Bishop, DK *et al.* (1998). Enhanced T cell engraftment after retroviral delivery of an antiviral gene in HIV-infected individuals. *Proc Natl Acad Sci USA* **95**: 1201–1206.
31. Schmidt, M, Zickler, P, Hoffmann, G, Haas, S, Wissler, M, Muessig, A *et al.* (2002). Polyclonal long-term repopulating stem cell clones in a primate model. *Blood* **100**: 2737–2743.
32. Ahr, B, Robert-Hebmann, V, Devaux, C and Biard-Piechaczyk, M (2004). Apoptosis of uninfected cells induced by HIV envelope glycoproteins. *Retrovirology* **1**: 12.
33. Primate Society of Japan (1986). Guiding principles for animal experiments using nonhuman primates. *Primate Res* **2**: 111–113.
34. Honjo, S (1985). The Japanese Tsukuba Primate Center for Medical Science (TPC): an outline. *J Med Primatol* **14**: 75–89.
35. Akiyama, H, Ido, E, Akahata, W, Kuwata, T, Miura, T and Hayami, M (2003). Construction and *in vivo* infection of a new simian/human immunodeficiency virus chimera containing the reverse transcriptase gene and the 3' half of the genomic region of human immunodeficiency virus type 1. *J Gen Virol* **84**(Pt 7): 1663–1669.
36. Lee, JT, Yu, SS, Han, E, Kim, S and Kim, S (2004). Engineering the splice acceptor for improved gene expression and viral titer in an MLV-based retroviral vector. *Gene Ther* **11**: 94–99.
37. Verzeletti, S, Bonini, C, Marktel, S, Nobili, N, Ciceri, F, Traversari, C *et al.* (1998). Herpes simplex virus thymidine kinase gene transfer for controlled graft-versus-host disease and graft-versus-leukemia: clinical follow-up and improved new vectors. *Hum Gene Ther* **9**: 2243–2251.
38. Ageyama, N, Kimikawa, M, Eguchi, K, Ono, F, Shibata, H, Yoshikawa, Y *et al.* (2003). Modification of the leukapheresis procedure for use in rhesus monkeys (Macaca mulata). *J Clin Apher* **18**: 26–31.

Supplementary Information accompanies this paper on the Molecular Therapy–Nucleic Acids website (http://www.nature.com/mtna)

OPEN

Nanogel-based pneumococcal surface protein A nasal vaccine induces microRNA-associated Th17 cell responses with neutralizing antibodies against *Streptococcus pneumoniae* in macaques

Y Fukuyama[1], Y Yuki[1,2], Y Katakai[3], N Harada[4], H Takahashi[5], S Takeda[5], M Mejima[1], S Joo[1], S Kurokawa[1], S Sawada[5], H Shibata[6], EJ Park[1], K Fujihashi[7], DE Briles[8], Y Yasutomi[6], H Tsukada[4], K Akiyoshi[5] and H Kiyono[1,2]

We previously established a nanosized nasal vaccine delivery system by using a cationic cholesteryl group-bearing pullulan nanogel (cCHP nanogel), which is a universal protein-based antigen-delivery vehicle for adjuvant-free nasal vaccination. In the present study, we examined the central nervous system safety and efficacy of nasal vaccination with our developed cCHP nanogel containing pneumococcal surface protein A (PspA-nanogel) against pneumococcal infection in nonhuman primates. When [^{18}F]-labeled PspA-nanogel was nasally administered to a rhesus macaque (*Macaca mulatta*), longer-term retention of PspA was noted in the nasal cavity when compared with administration of PspA alone. Of importance, no deposition of [^{18}F]-PspA was seen in the olfactory bulbs or brain. Nasal PspA-nanogel vaccination effectively induced PspA-specific serum IgG with protective activity and mucosal secretory IgA (SIgA) Ab responses in cynomolgus macaques (*Macaca fascicularis*). Nasal PspA-nanogel-induced immune responses were mediated through T-helper (Th) 2 and Th17 cytokine responses concomitantly with marked increases in the levels of miR-181a and miR-326 in the serum and respiratory tract tissues, respectively, of the macaques. These results demonstrate that nasal PspA-nanogel vaccination is a safe and effective strategy for the development of a nasal vaccine for the prevention of pneumonia in humans.

INTRODUCTION

Streptococcus pneumoniae is a major cause of bacterial infections throughout the world and is involved in the induction of a wide variety of infectious diseases, including otitis media, pneumonia, bacteremia, and meningitis in children and adults. This organism is usually a commensal bacterium in the upper respiratory tract of humans. Currently, four pneumococcal vaccines, 7-, 10- and 13-valent polysaccharide conjugate vaccines (PCV7, 10, 13) for children and a 23-valent pneumococcal polysaccharide vaccine (PPV23) for adults, have been developed for public use and are delivered by intramuscular injection.[1–3] However, as the conjugate vaccine does not protect against other capsular types, it provides little or no protection against total colonization with pneumococci.[4,5] The extensive carriage by other pneumococcal capsular types has led to strain replacement in disease with strains of non-conjugate vaccine capsular types.[6,7]

[1]Division of Mucosal Immunology, The Institute of Medical Science, The University of Tokyo, Minato-ku, Tokyo, Japan. [2]International Research and Development Center for Mucosal Vaccine, The Institute of Medical Science, The University of Tokyo, Minato-ku, Tokyo, Japan. [3]Corporation for Production and Research of Laboratory Primates, Tsukuba, Ibaraki, Japan. [4]PET Center, Central Research Laboratory, Hamamatsu Photonics K.K., Hamamatsu, Shizuoka, Japan. [5]Department of Polymer Chemistry, Kyoto University Graduate School of Engineering, Nishikyo-ku, Kyoto, Japan. [6]Tsukuba Primate Research Center, National Institute of Biomedical Innovation, Tsukuba, Ibaraki, Japan. [7]Departments of Pediatric Dentistry and Microbiology, The Immunobiology Vaccine Center, The University of Alabama at Birmingham, Birmingham, Alabama, USA and [8]Department of Microbiology, The University of Alabama at Birmingham, Birmingham, Alabama, USA. Correspondence: Y Yuki or H Kiyono (yukiy@ims.u-tokyo.ac.jp or kiyono@ims.u-tokyo.ac.jp)

Received 1 June 2014; accepted 2 January 2015; advance online publication 11 February 2015. doi:10.1038/mi.2015.5

The development of effective protein-based vaccines, which have the potential to provide better coverage for all strains, and to protect against colonization with all strains requires a thorough understanding of the roles and relative contributions to pathogenesis of the various putative virulence proteins. The pneumococcal surface protein A (PspA) is a well-known highly immunogenic surface protein of *S. pneumoniae* and is considered to be a promising vaccine candidate.[8,9] It is present on virtually all strains of pneumococci, and PspA-based vaccines against *S. pneumoniae* induce cross-reactive Abs in mice[10,11] and humans.[12] Moreover, PspA-specific mucosal and serum Abs responses are induced, and these responses are mediated by both Th1- and Th2-type cytokine production by $CD4^+$ T cells in infant mice via maternal immunization,[13] as well as in aged mice.[14] These findings indicate that PspA is a potent antigen for the development of effective pneumococcal vaccines not only in adults but also in children and the elderly.

S. pneumoniae commonly colonizes the nasal cavity, which can be protected by mucosal IgA.[15–17] Nasal vaccination induces effective mucosal immune responses in the respiratory tract, where initial bacterial and viral infections commonly occur; it could therefore be an effective immunization strategy for delivering protection from pneumococcal infection. However, most subunit type vaccines are poor immunogens for the induction of antigen-specific immune response in both systemic and mucosal immune compartments when nasally administered. Thus, the co-administration of biologically active mucosal adjuvants (e.g., cholera toxin and heat-labile toxin) or a better delivery system is needed to overcome the disadvantages of nasal antigen exposure. However, there are currently no safe nasal adjuvants or delivery systems, as evaluated by safety pharmacology studies, such as absorption, distribution, metabolism, and excretion in preclinical studies.

To overcome these concerns, we recently developed an effective vaccine delivery system with a self-assembled nanosized hydrogel (nanogel), which is composed of a cationic type of cholesteryl group-bearing pullulan (cCHP).[18] This cCHP nanogel efficiently delivers an antigen to epithelial cells in the nasal cavity, as well as to dendritic cells (DCs) under the basement membrane, and induces antigen-specific immune responses as an adjuvant-free vaccine.[19,20] Furthermore, a radioisotope counting assay showed that nasally administered cCHP nanogel carrying the [^{111}In]-labeled non-toxic subunit of botulinum neurotoxin does not accumulate in parts of the central nervous system (CNS) in mice.[19] In our separate study, we demonstrated that a nasally administered PspA-nanogel vaccine is safe and induces strong antigen-specific systemic and mucosal Ab immune responses, which can protect mice from invasive challenge with *S. pneumoniae*.[21]

MicroRNAs (miRNAs) have emerged as important regulators of many biological processes associated with the immune system, including the function of both innate and adaptive immune responses.[22–24] Accumulating evidence indicates that miRNA has an essential role in eliciting immune responses. For example, mice with T lymphocytes in which the endoribonuclease dicer, which is critical for miRNA biogenesis, has been conditionally knocked out show impaired thymic development and diminished Th-cell differentiation.[25,26] Dicer deficiency in B cells also prevents B-cell development.[27] These findings indicate the critical functions of miRNAs in the biology of the cells that constitute the immune system, such as in the development and differentiation of lymphocytes. Therefore, it is important to identify the miRNA biomarkers that engage in both mucosal and systemic antibody responses induced by nasal immunization with PspA-nanogel. Together, better understanding of the precise engagement of miRNAs in mediating humoral and protective immunity will be beneficial for the development of effective mucosal vaccines.

Before pursuing a clinical trial of a PspA-nanogel-based vaccine, we designed experiments to assess its safety for the CNS and its immunological efficacy, including immunologically relevant miRNA expression, and to demonstrate its safety and efficacy in nonhuman primates.

RESULTS

[^{18}F]-PspA-nanogel is retained for a long time in the nasal cavity but is not deposited in the olfactory bulbs or brain after nasal administration in macaques

We initially confirmed the physicochemical characterization of PspA-nanogel vaccine used in this study (**Supplementary Figure S1** online), and then investigated the retention of nasal PspA-nanogel in the nasal cavity and its accumulation in the olfactory bulbs and CNS in nonhuman primates by using three naive rhesus macaques. Because the results were nearly identical for the three macaques, we show the results for only one of the macaques in **Figure 1** (primate #1). The macaque's head was placed in the positron emission tomography (PET) scanner system and real-time imaging was performed for 6 h. To confirm the exact position of the cerebrum, we performed a magnetic resonance imaging (MRI) scan and then superimposed the PET images onto the MRI images. The real-time PET images clearly showed that nasally administered [^{18}F]-PspA-nanogel was effectively delivered to the nasal mucosa and retained in the nasal tissues for up to 6 h (**Figure 1a,c**). In contrast, most of the free form of [^{18}F]-PspA without a nanogel had disappeared from the nasal cavity by 3 h after nasal administration (**Figure 1a**). Furthermore, no deposition of [^{18}F]-PspA was detected in the cerebrum or olfactory bulbs of macaques, even 6 h after nasal administration (**Figure 1b**). These results show that PspA-nanogel is a CNS-safe and effective nasal vaccine delivery system in nonhuman primates.

Nasal vaccination with PspA-nanogel induces mucosal and systemic Ab responses in macaques

We next examined whether the nasal PspA-nanogel vaccine induced PspA-specific immune responses in cynomolgus macaques (primates #2-#9). One week after the final immunization, PspA-specific serum IgG Ab responses were significantly increased in macaques nasally immunized with 25 μg of PspA-nanogel when compared with macaques immunized with PspA alone or PBS only (**Figure 2a**). Examination of the longevity of PspA-nanogel-induced serum antigen-specific IgG

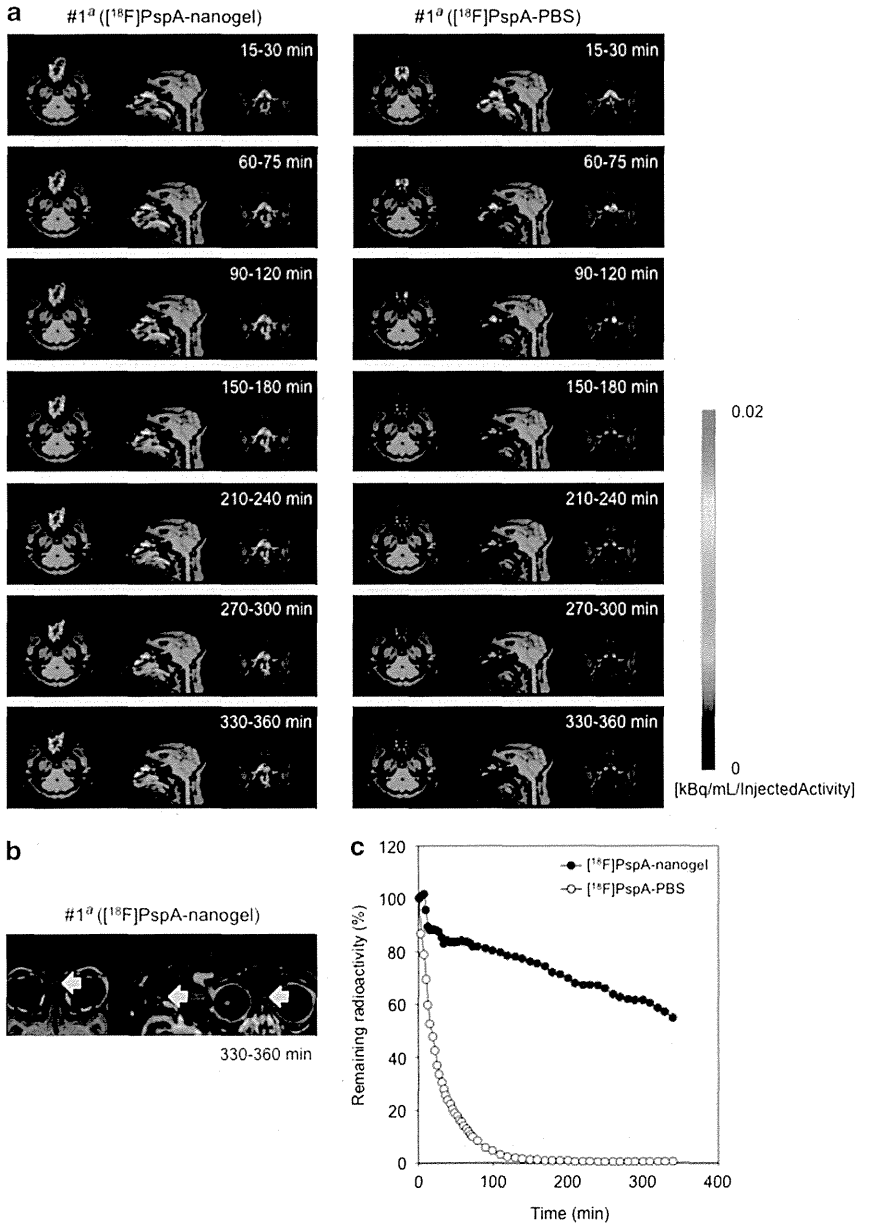

Figure 1 PET/MRI images (**a**,**b**) and TACs (**c**) for nasal administration of [^{18}F]-PspA-nanogel or [^{18}F]-PspA-PBS in a naive rhesus macaque. (**a**) After nasal administration of [^{18}F]-PspA-nanogel or [^{18}F]-PspA-PBS, the macaque's head was scanned for 6 h with a PET scanner. Real-time PET images overlaid on MRI images are shown for the indicated times post-administration. (**b**) To further check whether [^{18}F]-PspA accumulated in the CNS or olfactory bulbs (indicated by arrowheads), PET images taken at 6 h post-administration of [^{18}F]-PspA-nanogel were enlarged. (**c**) TACs for the nasal cavity for 6-h period after nasal administration of [^{18}F]-PspA-nanogel or [^{18}F]-PspA-PBS are presented. The data are expressed as percentages of the dose remaining after nasal administration. *a*: The same macaque was nasally administered of [^{18}F]-PspA-nanogel or [^{18}F]-PspA-PBS with a 1-week interval between administrations. CNS, central nervous system; MRI, magnetic resonance imaging; PET, positron emission tomography; TACs, time-activity curves.

Ab titers revealed that Ab levels gradually decreased over a period of 8 months in macaques nasally immunized with PspA-nanogel. Similarly, PspA-specific bronchoalveolar lavage fluid (BALF) IgG and nasal wash IgA Ab responses exhibited higher levels in macaques nasally immunized with PspA-nanogel when compared with macaques nasally immunized with PspA alone or PBS only (**Figure 2b,c**), and these Ab levels were also gradually decreased. In addition, PspA-specific BALF IgA Ab responses were slightly increased in two of the immunized macaques (#3 and #5) (**Figure 2c**).

When these macaques were given a dose of nasal booster of PspA-nanogel 9 months after the final immunization, the levels of PspA-specific serum and BALF IgG and nasal wash IgA Ab responses immediately recovered to those observed at 9 weeks